PREPARATION AND CHARACTERIZATION OF HYBRID ORGANIC−INORGANIC NANO COMPOSITE COATING

AMMAR SHAFAAMRI

DISSERTATION SUBMITTED IN PARTIAL FULFILMENT OF THE REQUIREMENTS FOR THE DEGREE OF MASTER OF TECHNOLOGY

FACULTY OF SCIENCE

UNIVERSITY OF MALAYA

KUALA LUMPUR

MALAYSIA

2015

DECLARATION

I hereby declare that the research work reported in this dissertation is my own unless specified and duly acknowledged by quotation.

_____

AMMAR SHAFAAMRI

2015

UNIVERSITI MALAYA

ORIGINAL LITERARY WORK DECLARATION

Name of Candidate: **AMMAR SHAFAAMRI** (I.C/Passport No: **000145753**)

Registration/Matric No: **SGG 130001**

Name of Degree: **MASTER OF TECHNOLOGY (M.Tech)**

Title of Project Paper/Research Report/Dissertation/Thesis ("this Work"):

PREPARATION AND CHARACTERIZATION OF HYBRID ORGANIC−INORGANIC NANO COMPOSITE COATING

Field of Study: **Advanced Materials**

I do solemnly and sincerely declare that:

(1) I am the sole author/writer of this Work;
(2) This Work is original;
(3) Any use of any work in which copyright exists was done by way of fair dealing and for permitted purposes and any excerpt or extract from, or reference to or reproduction of any copyright work has been disclosed expressly and sufficiently and the title of the Work and its authorship have been acknowledged in this Work;
(4) I do not have any actual knowledge nor do I ought reasonably to know that the making of this work constitutes an infringement of any copyright work;
(5) I hereby assign all and every rights in the copyright to this Work to the University of Malaya ("UM"), who henceforth shall be owner of the copyright in this Work and that any reproduction or use in any form or by any means whatsoever is prohibited without the written consent of UM having been first had and obtained;
(6) I am fully aware that if in the course of making this Work I have infringed any copyright whether intentionally or otherwise, I may be subject to legal action or any other action as may be determined by UM.

Candidate's Signature Date:

Subscribed and solemnly declared before,

Witness's Signature Date:

Name:

Designation:

ACKNOWLEDGEMENT

In the name of Allah, the Most Gracious and the Most Merciful

Alhamdulillah, all praises to Allah for the strengths and His blessing in completing this work. First and foremost, my most sincere and profound appreciation to my supervisor, Dr. Ramesh Kasi and Professor Dr. Ramesh A/L T. Subramaniam, who have supported me throughout my thesis with their patience and knowledge. I attribute the level of my Master degree to their encouragement and effort and without them this work would not have been completed. One simply could not wish for a better or friendlier supervisors.

A special word of thanks goes to Dr. Vengadaesvaran A/L V. Balakrishnan. The smooth running of the laboratory work is much more a testament to his efforts than my own. Many thanks also go to Dr. Ghassan and my lab mate Vikneswaran for the great support and advises.

I would also to take the opportunity to express my appreciation and thanks to my friends, namely Jad, Maher, Yamen, Hassan, Ghassan and Mohanad.

Last but not least, my deepest gratitude goes to my beloved my mother, sisters and my brother for their endless love, prayers and encouragement. Also not forgetting my brothers in law for supporting me in countless ways.

To those who indirectly contributed in this research, your kindness means a lot to me

Thank you very much.

ABSTRACT

The objective of the present work is to develop organic-inorganic nanocomposite coatings based on epoxy resin and hydroxyl-terminated polydimethylsiloxane (PDMS). The developed PDMS-epoxy polymeric matrix was used as the host for various weight percentages of reinforcement nanoparticles namely SiO_2 and ZnO. The employment of organic and inorganic functionalities into a single coating system provides a unique combination of distinctive properties. In this work, embedding nano-sized particles within the polymer matrix was carried out by utilizing the solution intercalation method. After that, the influence of the nanoparticles in enhancing the overall anticorrosion performance and the hydrophobicity properties were investigated. The electrochemical, thermal, structural and wettability properties of PDMS-epoxy nanocomposites have been examined. The results showed that that the coating system with 2 wt.% SiO_2 exhibited the most pronounced improvement. Same observation was related to the system reinforced with 2 wt.% ZnO nanoparticles. Superior corrosion resistance (R_c) with approximately 1 x 10^{11} Ω after 30 days of immersion in 3% NaCl solution was recorded. Nanocomposite coatings with hydrophobic characters were successfully achieved by increasing the surface roughness of the coated sample. Furthermore, the thermal studies of the archived systems reveal a good influence of the nanoparticles within the binder with no significant effects on the glass transition temperature.

ABSTRAK

Objektif utama kerja penyelidikan ini adalah untuk mencipta satu cat penyaduran yang mengandungi bahan komposit bersaiz nano dan satu system cat yang terdiri daripada bahan organic seperti epoxy dan bukan organik seperti polydimethylsiloxane (PDMS). Kombinansi bahan organik dan bukan organik dalam cat akan menyediakan satu siri cat yang mempunyai ciri-ciri unik yang tersendiri. Dalam kerja penyelidikan ini, dua jenis partikel bersaiz nano iaitu SiO_2 dan ZnO ditambahkan dengan kadar nisbah berat berbeza sebagai "reinforcement fillers" untuk meninggikan taraf kebolehbasahan air dan taraf tahan pengkaratan dimana kesemua sifat ini dikaji dengan terperinci. Selain daripada itu sifat serta ciri-ciri cat seperti sifat elektokimia, sifat tahan haba, sifat kebolehbasahan dan sifat fizikal PDMS-epoksi nanokomposit telah dikaji. Keputusan ujian sampel menunjukkan bahawa partikel bersaiz nano dengan 2 wt.% SiO_2 menunjukkan rintangan yang terbaik daripada tahan karat bagi tempoh rendaman yang tinggi iaitu 1×10^{11} Ω selepas 30 hari dengan rendaman dalam 3% NaCl. System cat yang mempunyai dua jenis nano komposit menunjukkan sifat tahan kebahasan yang tinggi.

Table of Contents

CONTENT **PAGE**

Table of Contents

List of Figures

List of Tables

Chapter 1: Introduction

Corrosion is critical for each country, therefore, the effect of this phenomenon must be considered as one of the economic factors due to the enormous losses caused by corrosion. All industries such as oil and gas, chemical, fertilizer, food, construction and marine mostly use metals in their products, operation tools and machines. Therefore, the storage conditions or working place environments, usually make these metals vulnerable to the corrosive environment. That leads to the necessary to protect metal's surface and try to find the best cost effective methods for this purpose (E. Sharmin et al., 2004; K. Ramesh et al., 2013).

Protective coating is one of the most efficient and cheapest techniques to protect the metals from corrosion. Currently, the modern systems of coating are focusing on the needs of enhancing the overall performance of organic materials. As one of the most growing research areas in the protective coating development, collaboration between the inorganic materials with the organic once gained an immense interest to employ the features of both components to overcome corrosion. Coatings required such materials with outstanding mechanical, thermal and anticorrosive properties to stand against the adverse environmental conditions (Grundmeier et al., 2000; Heidarian et al., 2010; Huttunen-Saarivirta et al., 2013).

Furthermore, polymeric nano-reinforced coatings have attracted extensive research activities as a convenient method for corrosion and fouling protection of metal surfaces, especially for steel protection. The unique mechanical, chemical, and physical properties of the materials in nanoscale play an important role in enhancing the corrosion protection of the bulk-size materials. Also, better barrier performance will result in the miscible of nano-sized

particles within the polymer matrix by reducing the porosity and zigzagging the diffusion pathways in front of water molecules and aggregates (Shi et al., 2009).

Utilizing the nanocomposite in the protection coatings plays a vital role in improving the barrier performance of the organic coatings. Moreover, there are many significant advantages could be related to the use of the advanced nanostructured coatings as the improvement in the mechanical, optical, tribological, hydrophobicity and electrochemical properties that could be obtained by employ the nanocomposite in the corrosion protection industrial applications(F. Dolatzadeh et al., 2011; S. Zhang et al., 2003).

1.1 Objectives of the Research

In order to achieve excellent corrosion protection coatings for metals, especially steel as one of the most affected materials by corrosion, this study aims to develop a novel hybrid organic- inorganic nanocomposite protective coating. The main purpose of this research is to produce a polymeric coating based on epoxy resin with hydroxyl-terminated polydimethylsiloxane (PDMS) as a modifier. Then investigate the effects of the incorporation of nanoparticles on the overall performance of these coatings. In other words, our objectives can be summarized as follows:

1. To develop organic-inorganic nanocomposite coating system consists of epoxy and silicone with nanoparticles.
2. To study the effect of the nanoparticles on the wettability and electrochemical properties.
3. To evaluate the structure and thermal properties of the achieved nanocomposite coating systems.

1.2 Outline of the Dissertation

There are six chapters have been included in this dissertation and are presented in the following order:

Chapter 1: This section, introduction, contains the research background, objectives of this work, characterization techniques and the research outlines.

Chapter 2: Includes a short literature review about the materials and the methods.

Chapter 3: Under the title of experimental methods, this chapter explains the preparation of the samples, the development process of the nanocomposite coating systems and also includes the characterization techniques.

Chapter 4: Covers all the characterization results of the development coating systems, i.e., thermal, wettability, structure and electrochemical properties.

Chapter 5: This section gives overall discussion about all results. At the end, conclusion and some of the proposed future work have been presented in the chapter 6.

Chapter 2: Literature Review

2.1 Introduction

Corrosion is defined as " the physico-chemical interaction between a metal and its environment, which results in changes in the properties of the metal and which may often lead to impairment of the function of the metal, the environment, or the technical system of which these form a part" (ISO 8044-1986; Montemor, 2014).

This natural phenomenon was the reason behind the necessary to find protection methods could make the metals able to withstand against the corrosive environments. As one of the most useful and economical technique to achieve the desired protection, organic coating, has gained the researchers interest in the last few decades.

In this study, we aim to develop a hybrid organic - inorganic nanocomposite coating based on epoxy resin. Silicone as one of the most suitable modifiers for epoxy resin was used to form the polymeric matrix which then became the host for nanoparticles to form the nanocomposite coating.

2.2 Organic coatings

During the last decades, organic coating was used as a fundamental method to protect metals from corrosion. The mechanism of this protection is done by covering the metal's surface, i.e., steel and aluminum, with an organic film. That is recognized as a smart way to gain anti-corrosion characteristic without losing the mechanical properties of the metal.

Moreover, organic coating can introduce one or multiple requested surface properties in one step such as color, wear resistance, formability, noise reduction and electronic insulation (Grundmeier et al., 2000).

A significant capability of the organic materials to act as barrier against water and oxygen diffusion was the primary reason behind the interest of the intensive using of organic coatings. Nowadays, the improvement of the organic film's barrier properties is considered as one of the key challenges in the area of developing long-life service of anti-corrosion coatings (Heidarian et al., 2010; Huttunen-Saarivirta et al., 2013).

There are several reasons behind the difficulties in the development of a high-performance anticorrosive coating systems as shown in Figure 2.1. As well as the selection of the components is essential for the development of novel organic coatings. Also, a detailed knowledge about the interactions of these components and their advantages and limitations are necessary too. For example, understanding the complicated relation at the interface between the coating film and the substrate is required. However, selection of the binder system components like resin, pigments, solvents and additive would give opportunity to manipulate with several characteristics, such as electrochemical, mechanical, physical and thermal properties (Nguyen et al., 1991; Sørensen et al., 2009).

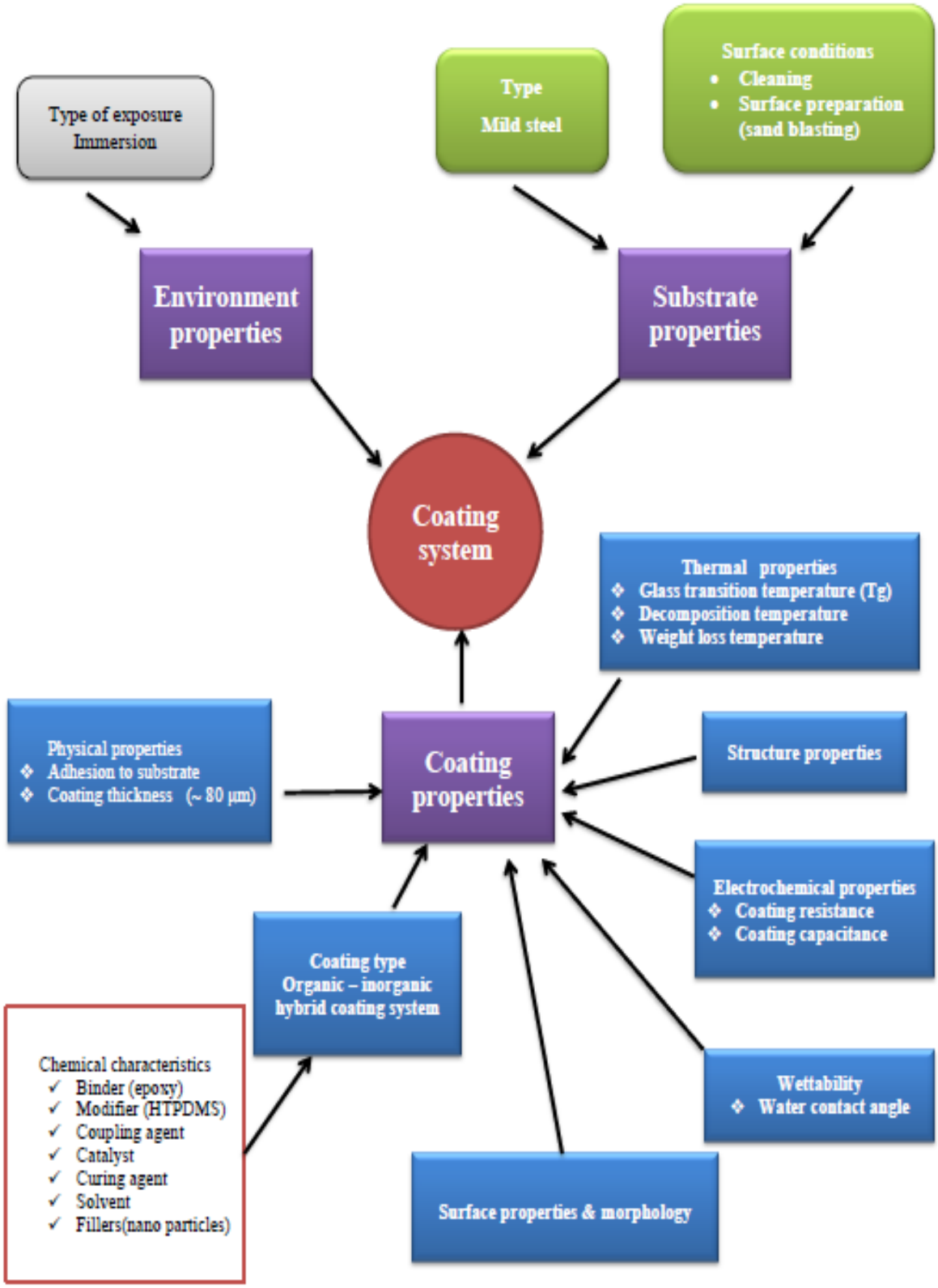

Figure 2.1: Factors affecting the durability of an anticorrosive coating system

2.3 Epoxy resins

Epoxy, as a member in the thermosetting polymers family usually produced by the reaction of an epoxide group (also called glycidyl, epoxy or oxirane group). This epoxide group is described according to the International union of pure and applied chemistry (IUPAC) and the chemical abstracts nomenclature as three membered cyclic ethers as shown in Figure 2.2. This ring structure of the epoxide act as a site for crosslinking with proton donors, i.e. amines or polyamides (Forsgren, 2006).

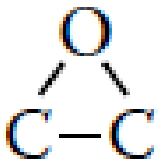

Figure 2.2: Epoxide or oxirane group

2.3.1 Classification of epoxy resins

First of all, the term "epoxy" may refer to a large variety of products that differ from each other. In fact, this diversity depends on the type of the group that epoxide group reacts with such as chloromethyl, carboxyl, hydroxyl, phenol, or amine group. Figure 2.3 (a) shows the three typical names that may epoxide group take. Whereas, the typical reactions of the epoxide group to form epoxies are shown in Figure 2.3 (b) (Forsgren, 2006; Wicks Jr et al., 2007).

a)

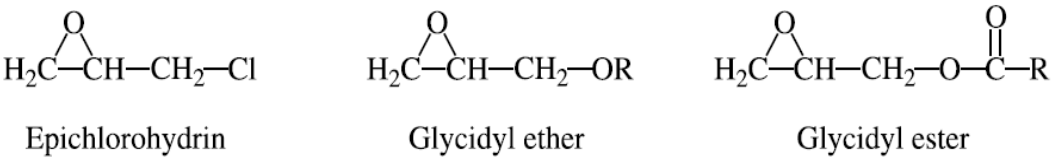

b)

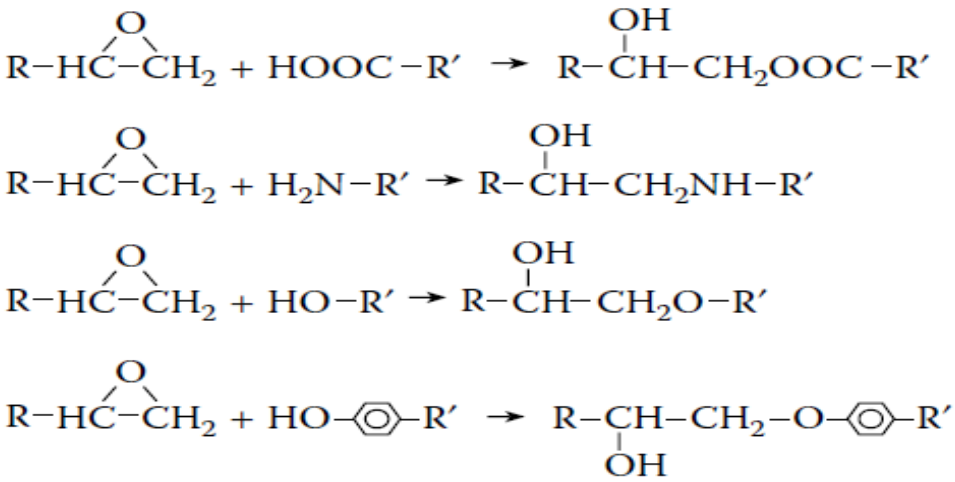

Figure 2.3: Epoxide group forms, (a) typical names of epoxide group and (b) the main reaction of the epoxide group

There are five main types of epoxy resins:

- Glycidyl ethers which is further classified as :
  - (DGEBA) Diglycidyl ethers of bisphenol - A
  - (DGEBF) Diglycidyl ethers of bisphenol - F
- Glycidyl esters
- Glycidyl amines
- linear aliphatic
- cycloaliphatic

- Bisphenol A Epoxy Resins

The most commonly utilized epoxy resins, and the first produced commercially, are those developed by condensing epichlorohydrin (1 - chloroprene 2 - oxide) with bisphenol A (bis 4 -hydroxyl phenylene - 2,2 propane) in the presence of sodium hydroxide. A detailed explanation of this reaction is well-documented in the literatures (Pascault & Williams, 2009; Wicks Jr et al., 2007).

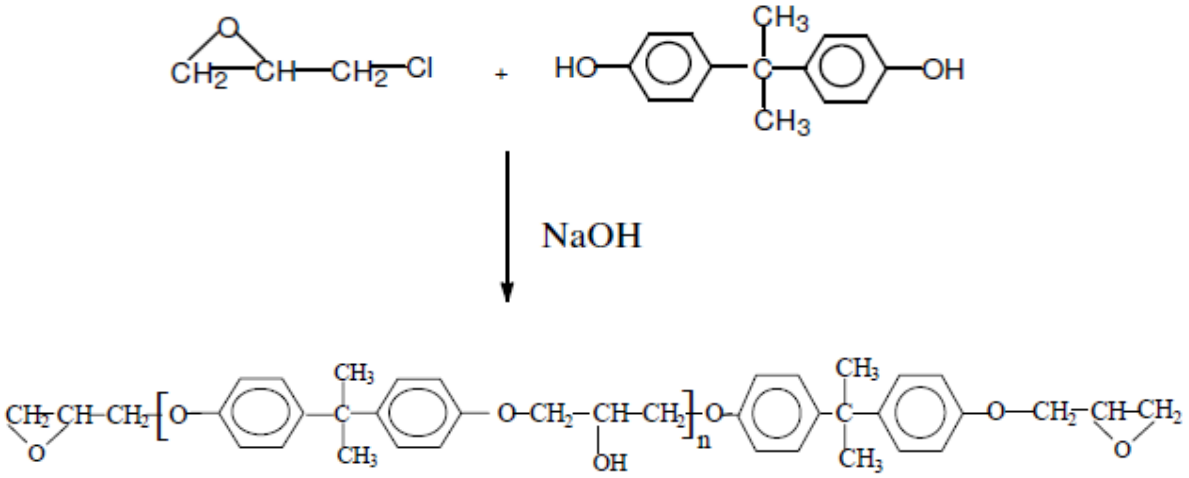

Figure 2.4: Synthesis method of DGEBA epoxy resin

In fact, bisphenol A epoxy resins could take different states according to the average value of the polymerization degree (n) that is shown in Figure 2.4. n value is ranging between 0 to 10. When n is close enough to zero; crystalline solid state is observed to the monomers at the room temperature. Whereas liquid state is matched to n values up to = 0.5, while amorphous solids exist for higher n values. Furthermore, functionality (F_n), number of epoxide groups per molecule, as well as epoxy equivalent weight (EEW) also consider as the most distinctive characteristics of epoxy resins. The epoxy equivalent weight (EEW) is described as the resin's weight in grams that contains one gram of the equivalent.

The intensive importance of identifying EEW comes from the use of this value to determine the exact amount of the curing agent that must be added to the resin to obtain materials with good physic-mechanical properties (Garcia & Soares, 2003; Pascault & Williams, 2009).

2.3.2 Properties of epoxy resins

Due to the characteristics of the epoxy resin, which is classified under thermosetting polymers, epoxy becomes one of the most materials used in last decades, and still the largest amount, in the organic coatings applications and industries. Low shrinkage, easy to handle, adhesiveness to most metals and alloys and the outstanding process ability make epoxy resin a required material in the anti-corrosion coatings. Moreover, excellent resistance to water, heat and chemicals, and the superior mechanical and electrical properties of epoxy resins as well as the ability to accept wide range of fillers and pigments made epoxy resin an attractive material to be study and develop for scientific and technological purposes.

However, like any other material, there are some shortcomings that related to the epoxy resins limit their usability. The inherent brittleness and the weak resistance against crack propagation result in facilitation in transfer water, oxygen and ions towards the coating/substrate interface which leads to accelerating the metal corrosion. Also, the poor hydrophobicity, weathering and impact strength are disadvantages in epoxy resins (Bagherzadeh & Mousavinejad, 2012; Hou et al., 2000; Huttunen-Saarivirta et al., 2013).

2.3.3 Epoxy curing system and curing agents

To achieve additional properties for epoxy resins, a process called ‘curing’ usually used in order to increase the molecular weight and reach the final properties of epoxy resins. This method includes the employment of curing agent that plays the significant role in

determining the final product properties. In other words, the chemical reactions occur during the curing period result in determining the morphology of the epoxy which, in turn, contributes in set the properties of the cured thermoset (Ghaemy & Riahy, 1996).

The curing for epoxy may be done according to one of the two general methods, catalyzed homopolymerization or by the incorporation with a cross-linking agent within epoxy network. In the catalyzed homopolymerization (also called ring-opening polymerization) curing system, just epoxide group will be involved in the polymer chain. Whereas, the using of incorporation method, also called bridging reaction, will lead to observing a copolymer consists of epoxy monomers and the cross-linking agent, called also as hardener or curing agent, composing the network (Dodiuk & Goodman, 2013).

There is a large variety of curing agents using for epoxy resins. The proper selection of the appropriate curing agent for a particular type of epoxy resin must take place first, and then the correct ratio of epoxy/ curing agent should be calculated with the attention for the suitable curing temperature. Some curing agents are listed below:

- Polyamides
- Primary and Secondary Aliphatic Amines
- Amine Adducts
- Cyclic Amines
- Aromatic Amines
- Acid-curing agents like Lewis acids, phenols, organic acids, carboxylic and acid anhydrides

2.4 Silicone

The silicones are classified as one of the polymeric materials and have been produced in a vast variety of forms. These products are ranging from fluids, which characterized with linear chain, to cross-linked network materials that in turn divided to rubber with slightly cross-linked structure and resins with highly cross-linked structure.

Pouget et al., (2009) mentioned that one of the reasons behind the importance of the silicon-based polymer in the industrial applications is due to the various forms of silicone molecular structure. Moreover, silicone materials have gained its interest according to the fact that their properties are strongly related to the structure which cannot find easily with another type of polymers.

Polydimethylsiloxane (PDMS) is one form of silicones materials. Figure 2.5 shows the structure of PDMS. Ananda Kumar & Sankara Narayanan, (2002) have developed a coating system based on the use of the Polydimethylsiloxane as a modifier for the epoxy resin which acts as the base in the system. This study confirmed an incensement in the thermal stability of the epoxy resin after the addition of the PDMS which was explained by Ananda Kumer & Sankara Narayanan, (2002) as a result of the inherent characteristic property of the siliconized epoxy coating system and the partial ionic nature of the silicone.

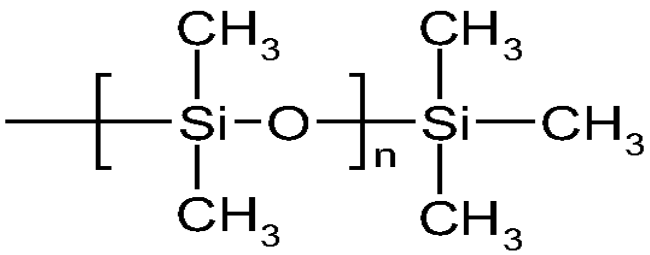

Figure 2.5: Polydimethylsiloxane (PDMS) structure

Moreover, a structure with a well dispersion of PDMS within the epoxy resin was achieved by (Ahmad et al., 2005). A superior thermal resistance, excellent physical-mechanical properties with high anticorrosive performance was confirmed as an enhancement of the epoxy by the addition of Polydimethylsiloxane (PDMS).

The most telling characteristics of silicone are the low surface energy and the excellent thermal and thermal-oxidative stability. The hydrophobic behavior of PDMS could result from a low surface energy character. Moreover, the Si-O-Si polymer backbone which surrounding with a polar methyl group can explain the hydrophobicity performance. In the other hand, Si-O bond has bond dissociation energy (BDE) equal to (110 kcal mol^{-1}) which is much higher than other formed bonds in the polymer chain like C- O, C-C and Si-C which have a BDE equal to 85.5, 82.6 and 76 kcal mol^{-1} respectively. This difference in the energy needed to the bond dissociation gives silicone the ability to withstand against the thermal effects and consider as material with excellent thermal stability (Pouget et al., 2009).

2.5 Nanocomposite coatings

Materials with at least one of their dimension in nanoscale are classified as nanosized or nanostructured materials. In nanoscale materials or in the nanocomposite, which has one of its component in the nano domain, parameters such as the size and distribution of the nano component (particle, grain, nanorods, etc.) within the matrix play very important role in determine the overall performance of the nanomaterials (Saji & Cook, 2012). Figure 2.6 shows the various types of nanomaterial.

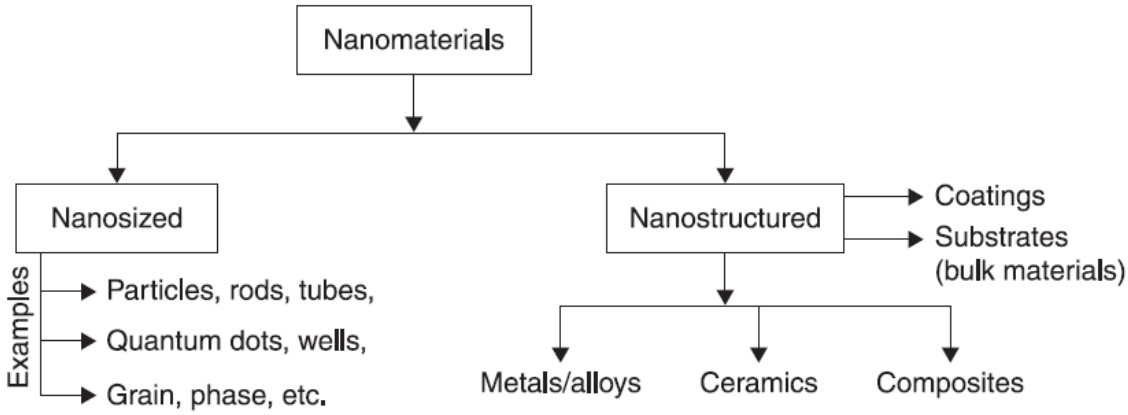

Figure 2.6: Types of nanomaterial (Saji & Cook, 2012)

Many decades ago, organic coatings have become a very efficient method for metals protection. Utilizing these coatings is a smart way to combine the mechanical properties of metals with the surface characteristics of the coatings (Grundmeier et al., 2000). However, the performance of coatings generally depends on their barrier properties and the good adhesion to the substrate (Akbarinezhad et al., 2008).The diffusion of water molecules and oxygen toward the metal surface and the permeability of the corrosive species through all polymers, due to a free volume micro-voids and high affinity between water and polar groups of polymers, are considered as shortcomings of these coating (González et al., 2001; Heidarian et al., 2011; Soer et al., 2009).

Polymeric nano-reinforced coatings have attracted extensive research activities as a convenient method for preventing corrosion and fouling of metal surfaces. The novel chemical, physical and mechanical properties of the materials in nanoscale play a significant role in the enhancement of the corrosion protection of the bulk sized materials also better barrier performance will result in the miscible of nano-sized particles within the polymer matrix, by reduce the porosity and zigzagging the diffusion pathway (Shi et al., 2009).

Silicon dioxide and Zinc oxide nanoparticles could be considered as the most commonly used inorganic nanoparticles, and they are multi-purpose nanoparticles that used to produce multifunctional nano coatings. They possess high hardness and low refractive index, hydrophobic enhancement and excellent dispersion with no aggregations (Dolatzadeh et al., 2011; Zhou et al., 2002). Despite that microscopic phase separation due to inhomogeneous dispersion of the inorganic nanoparticles within the organic matrix is considered as a major problem. Moreover, aggregation might take place during curing time even with a well distribution of the particles within the polymer matrix during the blending step. In addition, increment in viscosity could be observed with the higher percentage of nanoparticles result in a difficulty with coating applications (Amerio et al., 2008).

In this study, PDMS-epoxy nanocomposite coatings containing SiO_2 and ZnO nanoparticles separately at various concentrations have been successfully developed with the assistance of ultra-sonication process. The introducing of the nanoparticles into the polymer matrix was carried out by the employment of the solution intercalation method that based on dissolving the powder nanoparticles in a solvent such xylene through the mechanical stirring and sonication. After that, the prepared solution was mixed with prepolymer resulting from the blending process. Swollen have occurred in the nanoparticles due to the solvent exist then the polymer chains intercalated between the layers. The intercalated nanocomposite is obtained by solvent removal through vaporization. During the solvent evaporation, the entropy gained by the exit of solvent molecules from the interlayer spacing, allows the polymer chains to diffuse between the layers and sandwiching (Olad, 2011). The effects of nanoparticles addition within the polymer matrix on the wettability of the coating surface and its morphology were investigated. Determination the anti-corrosion properties and the

examination of the thermal properties of the coatings are also carried out, in order to provide information and understand the influence of SiO_2 and ZnO nanoparticles addition on the overall performance of the PDMS-epoxy matrix.

Chapter 3: Experiment methods

3.1 Introduction

Samples preparation and the methods that have been used to develop the hybrid organic-inorganic nanocomposite coating systems are described in this chapter. Moreover, the experiment methods and the fundamental principle of the characterization techniques which have been utilized to evaluate the performance of the coating films and to determine the properties of the developed nanocomposite coatings are also highlighted.

3.2 Preparation of the nanocomposite coatings

All chemicals, which have been used in this study, were used as received and without any further purification. Epoxy resin (EPIKOTE 828) formed from bisphenol A and epichlorohydrin was used as the base which was provided by Asachem, Malaysia with an epoxy equivalent of 184–190 and viscosity at 25°C between 12,000–14,000cP. Polydimethylsiloxane-hydroxyl-terminated (PDMS) with a viscosity of 750 cSt and density equal to 0.97 g/ml at 25 °C as a modifier and Dibutyltindilaurate as catalyst were both purchased from Sigma-Aldrich, Malaysia. Polyamide (EPICURE 3125) curing agent with an amine value of 330-360 mg/g was supplied by Asachem, Malaysia. The coupling agent used in this work was 3-Aminopropyltriethoxysilane (KBE-903) that obtained from Shin-Etsu Chemical Co. Ltd, Japan. Xylene (C8H10) was utilized as a solvent was obtained from Evergreen Engineering & Resources, Malaysia.

The nanocomposite coatings were prepared by using SiO_2 and ZnO nanoparticles with size of the particles of 10-20nm and 100nm respectively. The density of the Silicon dioxide nanoparticles was at 25 °C equal to 2.2-2.6 g/mL whereas, for Zinc oxide was estimated at 1.7 g/mL at 25 °C. Both types of used nanoparticles were purchased from Sigma-Aldrich, Malaysia.

Coatings were prepared by dissolving the nanoparticles for each SiO_2 and ZnO types separately in xylene at the weight ratio 8:2. This solution was then subjected to magnetically stirring at a rotation rate of 800 rpm for 30 minutes following by 15 minutes of sonicating. After that, 90 g of epoxy resin, 10 g of PDMS, stoichiometric equivalent of the coupling agent which was 3-aminopropyltriethoxysilane, 3-APS, (with the respect to OH group of HT-PDMS) and dibutyltindilaurate catalyst were mixed at 80 ◦C for 20 minutes with constant stirring. Different weight ratios of dissolved nanoparticles were added to the blend and mixed for 20 minutes at 1000 rpm rotation rate. 60 minutes of sonication process was done before the addition of the calculated percentage (w/w) of the polyamide. Constant stirring for 5 minutes was done out followed by subjecting the mixture to vacuum with the assist of vacuum pump to remove the trapped air bubbles and CH_3OH (side product of the reaction of PDMS and 3-APS). Table 3.1 shows the nanoparticles content in the prepared nanocomposites. A Flow chart of the nanocomposite coating preparation is shown in Figure 3.1.

Table 3.1: Nanoparticles content in the prepared nanocomposite coatings.

Epoxy (wt.%)	PDMS (wt.%)	SiO_2 Nanoparticles (wt.%)	ZnO Nanoparticles (wt.%)
100	-	-	-
90	10	2	-
90	10	4	-
90	10	6	-
90	10	8	-
90	10	-	2
90	10	-	4
90	10	-	6
90	10	-	8

3.3 Preparation of samples

All prepared coatings systems were applied on both sides of cold-rolled mild steel panels (obtained from GT Stainless, Melaka, Malaysia) with dimensions of 0.5 mm (thickness) × 50.0 mm (width) × 75.0 mm (length) by brushing method after being degassed under vacuum for 5 minutes. Any dust, dirt, oil, grease, etc. on the panels were cleaned before the coating application. The cleaning process was conducted using acetone for washing the panels and followed by sandblasting the specimens. The prepared coatings were also applied on Teflon plates. After coat the steel sheets as well as Teflon plates, all samples left to dry for two days under ambient condition then samples were subjected to heat treatment at 80 °C

for 24 h. The thickness of the coating films was controlled to be within the range of 70 µm to 80 µm monitored with a digital coating thickness gauge model Elcometer 456 (Figure 3.2).

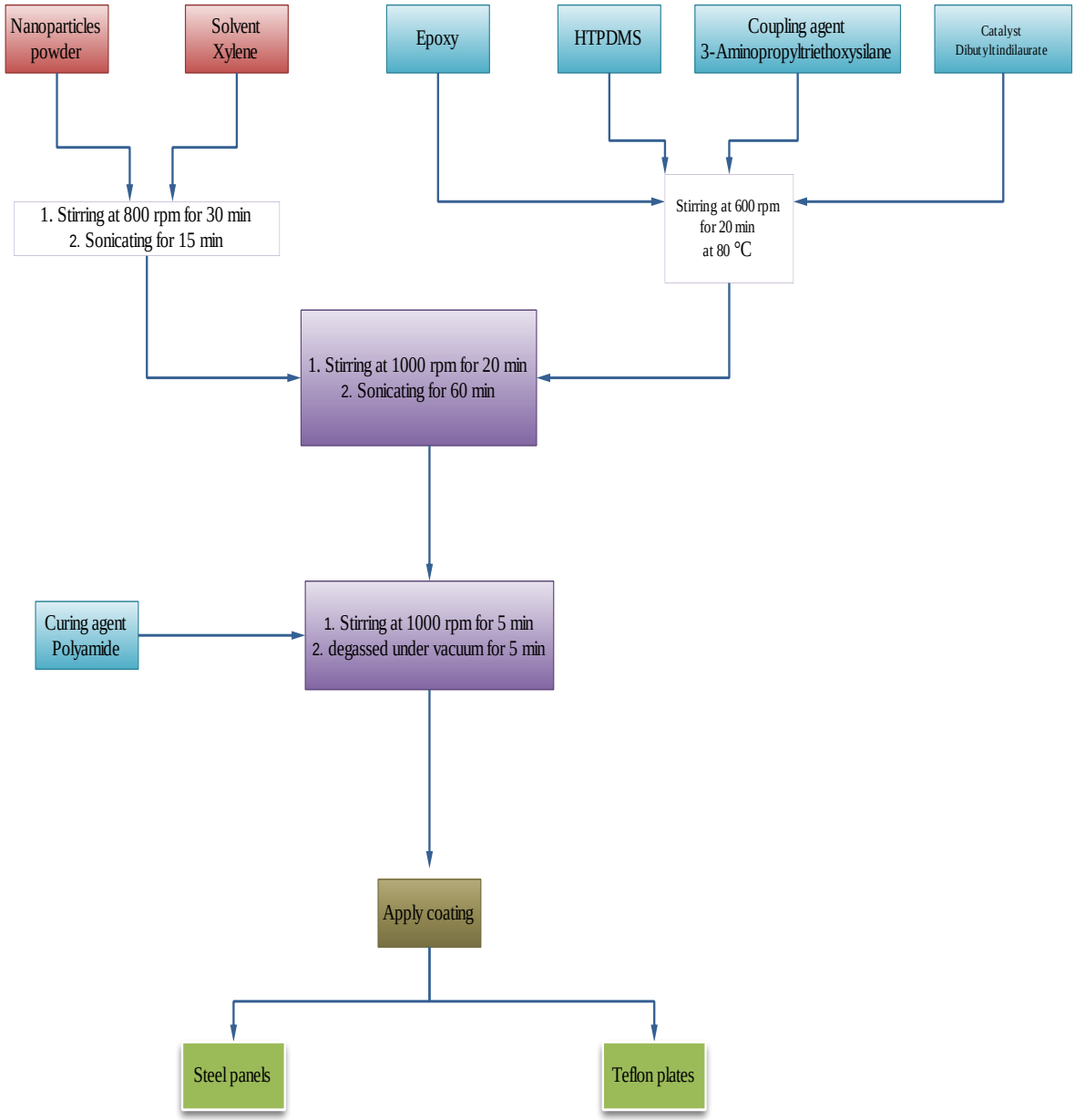

Figure 3.1: Flow chart of the nanocomposite coating preparation

Figure 3.2: Coating thickness gauge Elcometer 456

Fourier transform infra-red (FTIR) spectroscopy, Field Emission Scanning Electron Microscopy (FESEM), Water Contact Angle test (WCA), Electrochemical Impedance Spectroscopy (EIS), Differential Scanning Calorimetry (DSC) and Thermogravimetric analysis (TGA) were used to determine and evaluate the properties of the developed hybrid organic-inorganic nanocomposite coating systems.

3.4 Fourier Transform Infra-red (FTIR) Spectroscopy

FTIR is a very important technique and has been utilized widely in the coating industry. During the development of the organic coatings, determination of the bonding structure and complication characteristics could give a clear understanding of the cross-linking process between organic functional groups. Moreover, the appearance or absence of some absorption peaks in FTIR spectra can be used to confirm the complete curing of the blended resins. Fourier Transform Infra-red (FTIR) Spectroscopy was used to analyze the

chemical bonding structure and to determine the changes result from the cross-linking of epoxy/polyester hybrid coating system (Ramesh et al., 2013). Figure 3.3 shows a Schematic diagram of FTIR instrument.

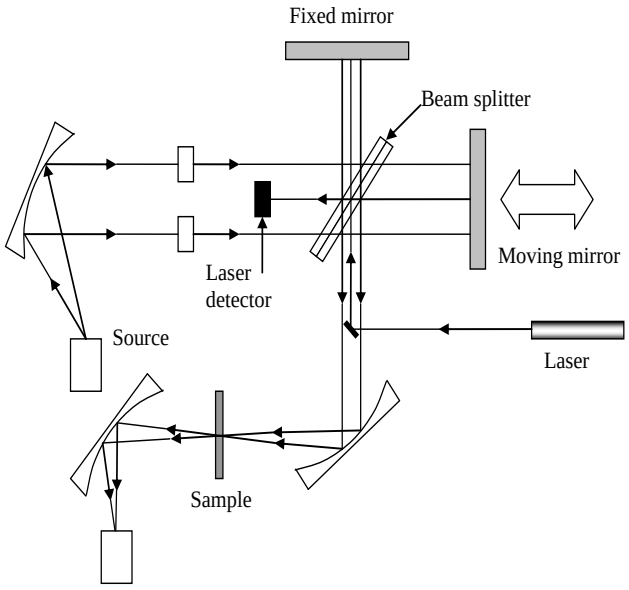

Figure 3.3: Schematic diagram of FTIR instrument configuration

In this study, Fourier transform infra-red (FTIR) spectra was used to analyse the changes in the molecular structure that may occur from blending epoxy resin with PDMS. The wavenumber spectrums in the region from 400 cm^{-1} to 4000 cm^{-1} with resolution of 4 cm^{-1} with a 32-scan data accumulation were investigated for identifying the presence of specific functional groups in the developed coating samples. The analyses were carried out using Nicolet iS10 spectrophotometer with OMNIC spectra software from Thermo Scientific (Figure 3.4).

Figure 3.4: FTIR spectrometer

3.5 Field Emission Scanning Electron Microscopy (FESEM)

In this study, FESEM has been used to study the morphology of the prepared samples and to identify the uniform dispersion of the nanoparticles within the polymer matrix. Cold rolled mild steel panels coated by brushing technique and heat treated at 80 °C for 24 h were tested by using FEI Quanta 450 FEG at 10 kv as accelerating voltage with the assist of low vacuum (LVSEM). Figure 3.5 shows the scanning electron microscope instrument with the FE gun and SDD EDS detector.

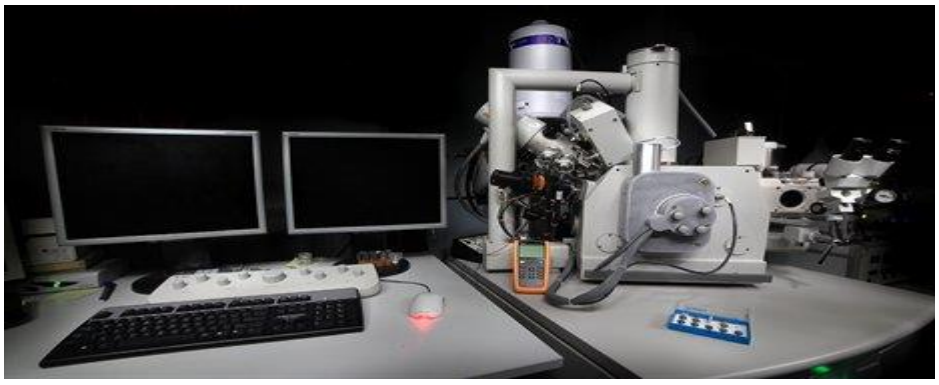

Figure 3.5: Field emission scanning electron microscope instrument

3.6 Water contact angle test

Hydrophilic, hydrophobic and super-hydrophobic are the terms that used to describe the state or the ability of one surface to be wet or not. Studying the phenomenon of wetting or non-wetting of a solid by a liquid, usually achieved by measuring the contact angle (θ°) of a liquid drop on the surface of the sample. Figure 3.6 shows the relation between the value of the contact angle and the wettability of the surface. While θ < 90° indicates a hydrophilic behavior of the surface, θ > 90° corresponds to a hydrophobic tendency. However, when θ becomes more than 150° the surface could classify as a super-hydrophobic surface.

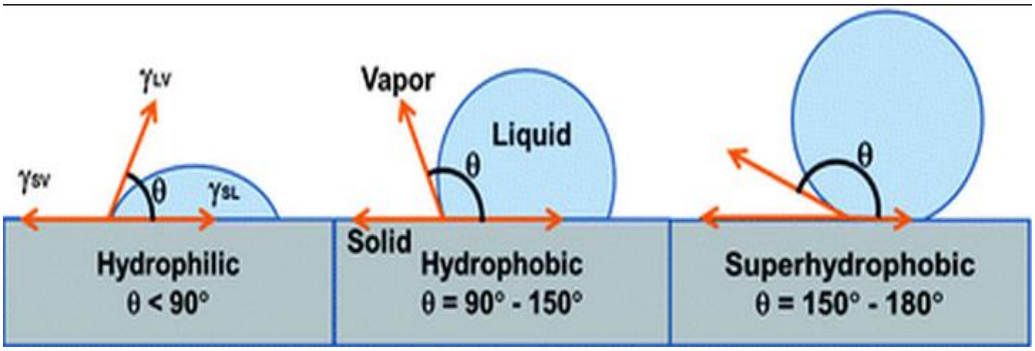

Figure 3.6: Relationship between contact angle and wettability properties

Kanungo et al., (2014) have used contact angle measurements to study the roughness effect on the wettability of rough PDMS surface. Moreover, Kapridaki & Maravelaki-Kalaitzaki, (2013) have utilized the determination of the static contact angle (θ°) to confirm that the hydrophobicity of the surface was enhanced by the methyl groups of Polydimethylsiloxane (PDMS).

Day after day, the potential applications of the hydrophobic surfaces, which have the capability to prevent liquid adhesion on surfaces and minimize the contact area between the

liquid and the metals, is increasing. In this study, the determination of the static contact angle (θ°) of the water drop on the surface of coated samples was carried out according to the sessile drop method. Figure 3.7 shows the video-based optical contact angle measuring system instrument, OCA 15EC (dataphysics, Germany) that was used to perform the measuring of the contact angle by using droplets of distilled water (~5 ml volume) under laboratory conditions. Five different places of each sample were subjected to this test with the using of needle located close enough to the tested surface which makes the kinetic energy of the droplets negligible. Capturing the images was done immediately for estimating the static contact angle (θ°).

Figure 3.7: Contact angle instrument

3.7 Electrochemical Impedance Spectroscopy (EIS)

Development of a new coating systems, determination of the best combination of organic resins to overcome the corrosive effect of a particular environment, study the properties that controlling the protection performance of the polymer coating film, as well as investigate the quality of the achieved coating systems and so on are some of the reasons behind the importance of electrochemical impedance spectroscopy as a fundamental tool to study the degradation of coatings in coating industries as well as for research purposes

In this work, electrochemical impedance spectroscopy has been used to investigate the anti-corrosion performance and the barrier properties of the developed organic-inorganic nanocomposite coatings. The measurements were carried out by using the three electrodes system that shown in Figure 3.8. The working electrode was the uncoated part of the samples and the exposed area was equal to 3 cm^2. Saturated calomel electrode was used as a reference electrode, and a platinum electrode served as a counter electrode. The frequency range of 0.1 Hz to 100 KHz was used to do the EIS tests in 3% NaCl solution at ambient condition.

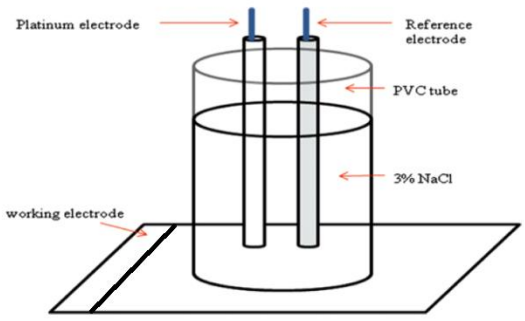

Figure 3.8: EIS test setup

Electrochemical impedance spectroscopy study was performed using a Gamry PC14G300 potentiostat (Gamry Instruments, Warminster, PA, USA) with a faraday cage to reduce the noise, shown in Figure 3.9, and Echem Analyst Version 6.03 analyzer for the results evaluation.

Figure 3.9: Electrochemical impedance spectroscopy instrument with faraday cage

3.8 Differential Scanning Calorimetry (DSC)

Differential scanning calorimetry (DSC) is a powerful technique to study the thermal properties for materials. The changes that take place in the polymer as it is heated or cooled and thermal transitions can be obtained by using DSC. The simple principle of testing the polymer coatings by using DSC is shown in Figure 3.10. The computer will control the heaters to perform a specific heat rate, but the heater below the sample pan will give more energy (heat) than the heater for the reference pan. This difference in the heat energy gives the ability to identify the amount of energy needed to heat the sample. In this study, DSC was used to investigate the thermal properties and determine the glass transition temperature (T_g) of the polymeric coating.

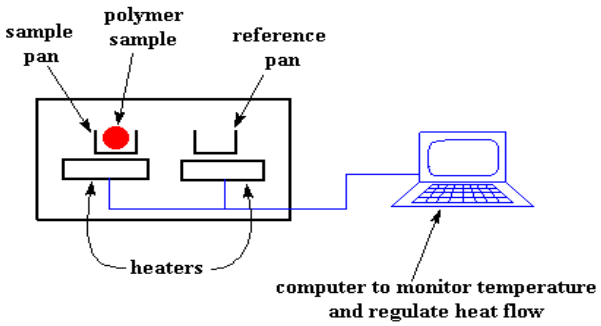

Figure 3.10: Differential scanning calorimetry equipment schematic

Glass transition temperature, crystallization, melting and heat capacity are classified as the most important information that can be obtained from DSC. These changes in the polymer can be caused by absorbing or releasing heat energy. The T_g is related to a specific volume change with the change in specific heat. While endotherm, indicates the heat absorption by the polymer and here where the crystallization happened. Melting transition occurs when the heat is released from the polymer, and that called exotherm. The main three transition characteristics are shown in Figure 3.11.

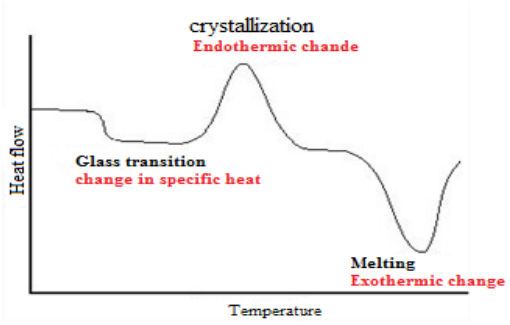

Figure 3.11: Typical DSC curve

The temperature of the transition from the amorphous glassy state to a rubbery state is defined as the glass transition temperature (T_g). Not all materials express this type of

transition which in turn can be related to the amorphous materials, glassy and semi crystalline polymers. Glass transition temperature (T_g) provides very important information in coating industry. Many of researchers used (T_g) to evaluate the performance of the coating systems that result from blending two or more polymers together. Kumar and Narayanan, (2002) confirmed the inter-cross-linked network structure for the siliconized epoxy coating system by observing a single glass transition temperature (T_g) for the binder.

In this research, an intra-cooler equipped thermal analysis (TA) instrument system, DSC TA-Q200 (Figure 3.12), was employed to determine the glass transition temperature (T_g) of the samples. The results were evaluated with the STARe software version TA Universal Analysis V4.7A. Samples with mass range between 10 mg to 12 mg were used for DSC measurements. Samples were scanned in hermetically sealed 40μL aluminium crucible in a self-generated atmosphere. The self-generated atmosphere was obtained by piercing a 50 μm hole on the aluminium lid of a sealed crucible. The DSC program ran dynamically under Nitrogen condition with a flow rate of 50 ml/min. The samples were tested with the following temperature program:

1) Heating the sample from - 50 ºC to 180 ºC at 10ºC/min

2) Cooling from 180 ºC to - 50 ºC at 10ºC/min

3) Heating from - 50 ºC to 180 ºC at 10ºC/min (the actual measurement)

Figure 3.12: Differential scanning calorimeter equipment

3.9 Thermogravimetric Analysis (TGA)

Thermogravimetric analysis (TGA) is one of the thermal analysis techniques that used to study the effect of the temperature changes in the mass of the sample. Moreover, time effect can also be studied by using (TGA) technique through utilizing a controlled temperature program in a controlled atmosphere. The typical temperature ranges for the TGA tests are from the ambient up to 1000 ºC. Thermogravimetric analysis provides reliable information about the polymer degradation temperature, residual solvent levels, absorbed moisture content and the amount of inorganic fillers in a polymer matrix for composite materials. Also, study the thermal stability and the thermal degradation of the polymer coatings have studied by TGA (Chew et al., 2000).

Kumar and Narayanan, (2002) have used TGA to determine temperatures at which 10, 20, 30 and 50% weight loss occurs for unmodified and hydroxyl terminated polydimethylsiloxane modified epoxy. From the TGA thermograph the thermal stability of the polymer and the efficient of the inorganic fillers or the modifiers in enhancing thermal degradation temperature can be investigated. Qualitatively, the higher the decomposition temperature, the greater is the stability. Simply mention, TGA curve can be extremely useful in revealing the purity of a polymer or resin.

Figure 3.13: Thermogravimetric analysis (TGA) equipment

In this study, TGA was carried out using a standard hardware and software integration options with Mettler Toledo TGAQ500 thermal gravimetric analyser (Instrument serial number: Q500-1448) and STARe software version TA Universal Analysis V4.7A (Figure 3.13).The measurements were carried out from 30ºC to 800ºC at a rate of heating equal to 50ºC/min under nitrogen gas flow rate of 60 ml/min and balance nitrogen gas flow rate of 40 mL/min. Samples with mass range between 10 mg to 11.80 mg were used for TGA measurement.

Chapter 4: Results

4.1 Introduction

This chapter covers all the results of characterizations that carried out on the coatings developed with epoxy only, 90:10 wt. % of epoxy : PDMS (binder coating), binder with nano SiO_2 nanocomposites and binder with nano ZnO nanocomposites. In addition, all the investigations and the experiments that took place, in order to examine the influence of the nanoparticles on the properties of the developed silicone modified epoxy, were reported.

4.2 Fourier Transform Infrared Spectroscopy (FTIR) studies

FTIR spectra for unmodified epoxy, silicone modified epoxy and the developed SiO_2 and ZnO nanocomposites are illustrated in Figure 4.1. The characteristic peaks and their assignments to the specific bonds are tabulated in Table 4.1. The spectrum of neat epoxy (Figure 4.1) shows an absorption peak at 915 cm^{-1} which represents the epoxy ring.

The crosslinking process among epoxy resin and PDMS, in the present of 3- APS coupling agent, leads to observing the fundamental change in the spectrum as opening the epoxy ring and the absent of its peak as shown in Figure 4.1. However, the appearance of the peaks at 803 cm^{-1} and 1090 cm^{-1} corresponded to the Si-C band and stretching of Si-O-Si bond respectively, considered as the evidence of the presence of silicone within the epoxy polymer chain and indicated that crosslinking occurred. These bands were not observed in the spectrum of neat epoxy but observed in all samples containing PDMS. The absorption peaks at 2924 cm^{-1} and 2853cm^{-1} are due to the asymmetric methyl group stretching confirming the

presence of Si–O–CH_3 and Si–$(CH_2)_3$ groups. No peak at 3500 cm^{-1} was observed in all spectra which in turn can confirm the absence of free OH group of the hydroxyl-terminated PDMS (Velan & Bilal, 2000).

Table 4.1. Characteristic Infrared Absorptions of developed coating systems

Absorption peak from literature	**Neat epoxy**	**PDMS/epoxy**	**SiO_2 Nanocomposites**	**ZnO Nanocomposites**	**Band assignment**
(cm^{-1})					
803 (Kapridaki & Maravelaki-Kalaitzaki, 2013; Téllez et al., 2004)	Not observed	803	803	803	Si-C Stretching
915 (Enns & Gillham, 1983; Kumar & Narayanan, 2002; Nikolic et al., 2010)	915	Not observed	Not observed	Not observed	Epoxy ring
1090 (S. Duo et al., 2008)	Not observed	1090	1090	1090	Si-O-Si asymmetric stretching
2850 (Kumar & Narayanan, 2002)	Not observed	2853	2853	2853	C-H stretching of Si–$(CH_2)_3$
2924 (Chen et al., 2003)	Not observed	2924	2924	2924	C-H stretching of Si–O–CH3

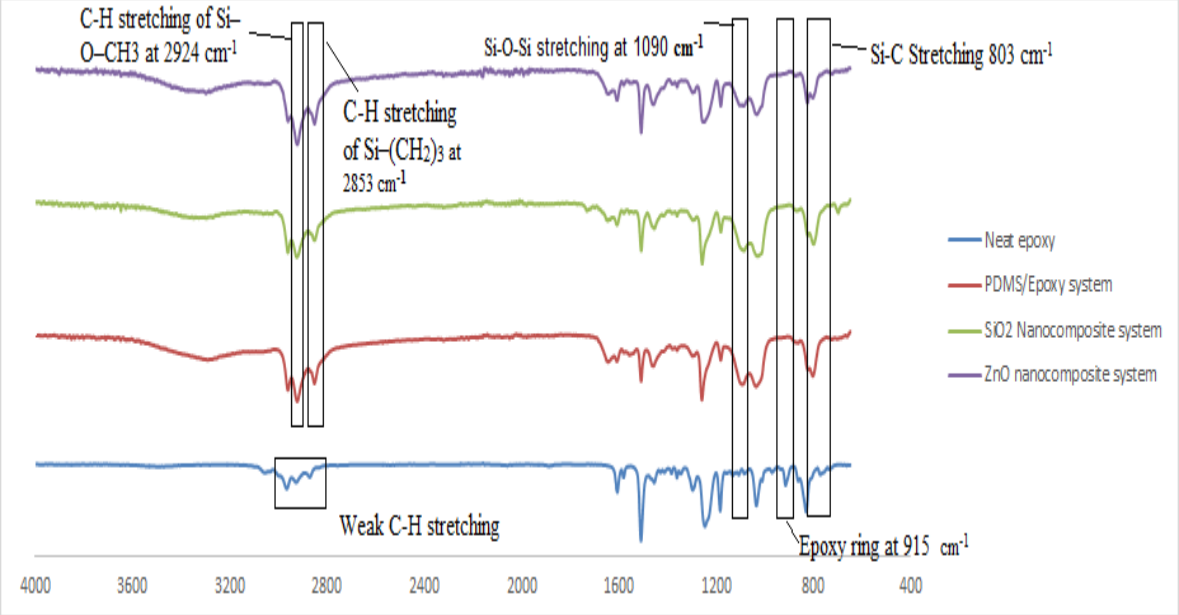

Figure 4.1: FTIR spectra of all coated samples

The development process of the hybrid organic- inorganic siliconized epoxy nanocomposite coating could divide into two main steps:

- Cross-linking process:

The production of a siliconized epoxy prepolymer was carried out by the employment of the 3-APS as a coupling agent in the present of catalyst. This process may be explained in two stages (Velan & Bilal, 2000):

Stage I: In this step, the reaction between the epoxy resin and the amino group of the 3-aminopropyltriethoxysilane coupling agent was occurred first in order to opening the epoxy ring as the following reaction.

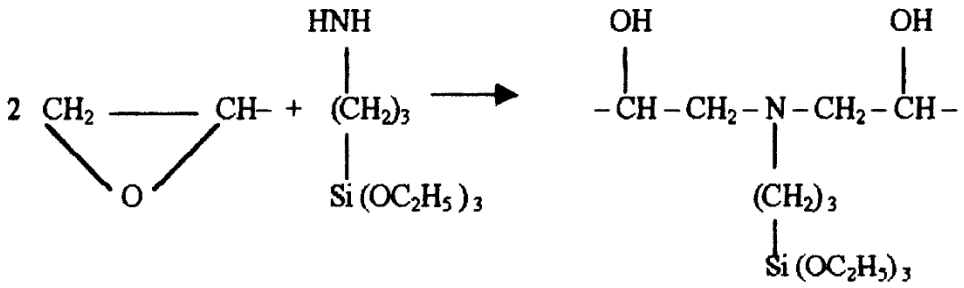

Figure 4.2: The reaction between the epoxy resin and the amino group of the coupling agent (step 1)

Stage II: Secondly, PDMS reacts with epoxy under the encouragement from the alkoxy group of 3-APS and the stimulation of the catalyst.

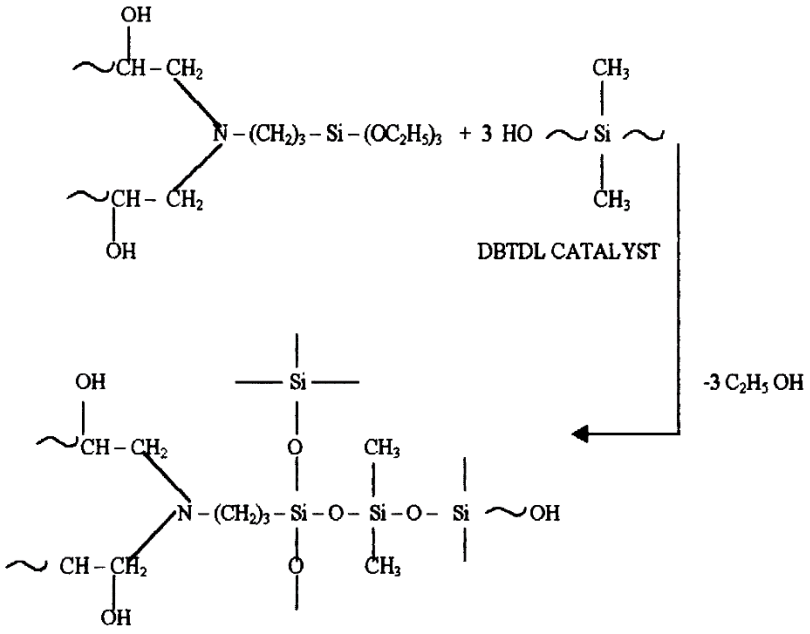

Figure 4.3: The reaction between the epoxy resin and PDMS with the present of the coupling agent and the catalyst (step 2)

- Curing process:

As well as the polyamide curing agent reacts with the major amount of the epoxy resin and opens the epoxide ring. Also, amino groups of polyamide react with the OH group results from the ring-opening reaction and of the hydroxyl groups of HT-PDMS.

Matin et al., (2015), Nikolic et al., (2010) and Ramezanzadeh et al., (2011) have studied the reaction between epoxy resin and polyamide curing agent and have concluded with that: three steps, or more could take place during the curing process. The first possible reaction is between the primary amine (NH_2) and the epoxide rings which in turns results in opening the ring. After that, creation of the tertiary amine takes place due to the reaction between the secondary amine (NH) group and another epoxide ring. In addition, other possible reactions are shown in Figure 4.4.

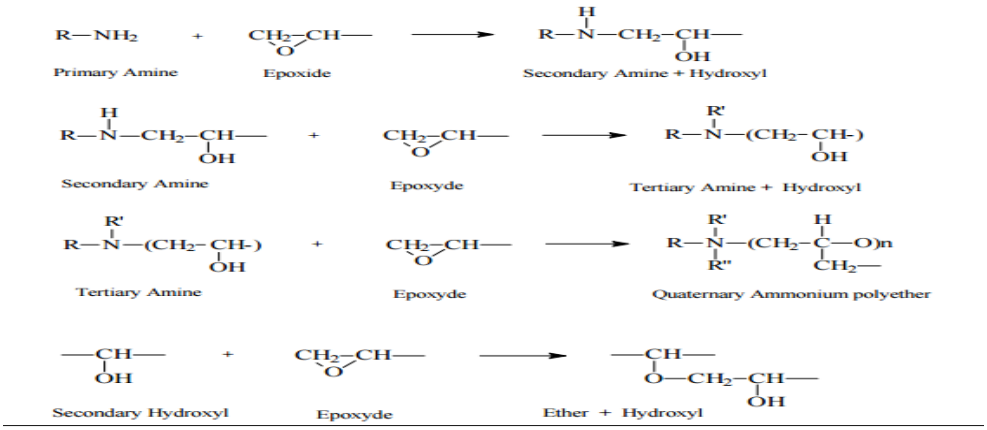

Figure 4.4: The possible reactions of the epoxy resin with polyamide curing agent (Nikolic et al., 2010)

It is worth to be mentioned that the results also indicated that the introducing of the nano SiO_2 and ZnO particles within the PDMS-epoxy polymeric matrix had caused insignificant changes in the structure of the all developed nanocomposite coating systems.

4.3 Water contact angle

In this work, water contact angle (WCA) measurement was used to investigate the effect of PDMS on the wettability of the epoxy resin. Furthermore, contact angle test was utilized also to determine the effectiveness of nanocomposite coatings containing SiO_2 or ZnO nanoparticles as hydrophobic coatings on the steel panels. The results, as shown in Table 4.2, indicate the hydrophilic nature of unmodified epoxy coatings with WCA of 65°.

In order to transfer the surface of the coated steel panel from hydrophilic surface to hydrophobic one, Jiang et al., (2000) and Wang et al., (2011) have pointed out that there are two main factors have to be considered to achieve an intensive hydrophobic improvement of the solid surface. First, the chemical composition plays a vital role in enhancing the hydrophobicity of the surface. That was confirmed by increasing the contact angle value after the application of PDMS-epoxy hybrid coating, which in turn can be attributed to the hydrophobic nature of PDMS with low surface energy. In order to develop a further hydrophobicity, the second factor that corresponded to the topographic structure of the surface was considered. Figures 4.5 and 4.6 show the influence of the PDMS as well as the nano fillers on the wettability of the coatings. Transformation from the hydrophilic state to hydrophobic one was observed, first due to the addition of polydimethylsiloxane (PDMS) into the epoxy resin. In addition, decrease the permeability of the coating film and enhancing the hydrophobicity characteristic were obtained by reinforcing the polymeric matrix with nano SiO_2 particles.

Table 4.2: Water contact angle on the steel panel surface coated with neat epoxy, PDMS-epoxy, SiO_2 nanocomposites and ZnO nanocomposites coating systems.

Water contact angle (θ°)

100 wt.% epoxy		10:90 wt.% **PDMS : Epoxy**	
65		**96**	
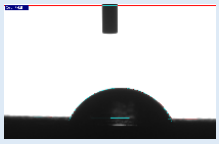			
2 wt.% SiO_2	**4 wt.% SiO_2**	**6 wt.% SiO_2**	**8 wt.% SiO_2**
122	**127**	**132**	**121**
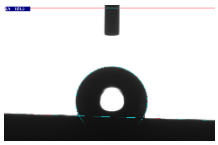	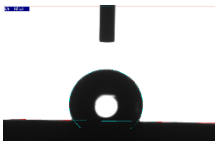	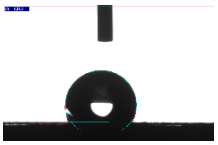	
2 wt.% ZnO	**4 wt.% ZnO**	**6 wt.% ZnO**	**8 wt.% ZnO**
119	**121**	**128**	**118**
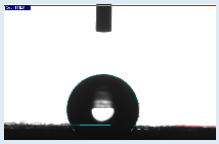	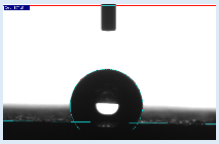		

The water contact angle, which is widely used to indicate the hydrophobicity of the coatings system, was increased by the increasing of addition amount of SiO_2 nanoparticles. The most pronounced effect was observed when 6 wt.% nano SiO_2 was used with a corresponded contact angle at 132°. (C. Su et al., 2006) have explained the effect of nano silica particles in improving the hydrophobicity of the epoxy coatings by the rough surface result from embedding SiO_2 particles within the coating film.

The same effect was observed when PDMS-epoxy matrix was reinforced with ZnO nano fillers. It was mentioned that, as the concentration of ZnO nanoparticles increases, the contact angle increases. That could impute to the roughness caused by embedding nano ZnO (Su et al., 2006). The most pronounced effect was also observed when 6 wt. % nano ZnO was used with a contact angle of 128°. On the other hand, further increase the concentration of nanoparticles either SiO_2, or ZnO type did not enhance the surface hydrophobicity anymore. This observation at high concentration of nanoparticles can be attributed due to the high tendency of the nanoparticles to form aggregations at high loadings ratio (Ramezanzadeh et al., 2011)

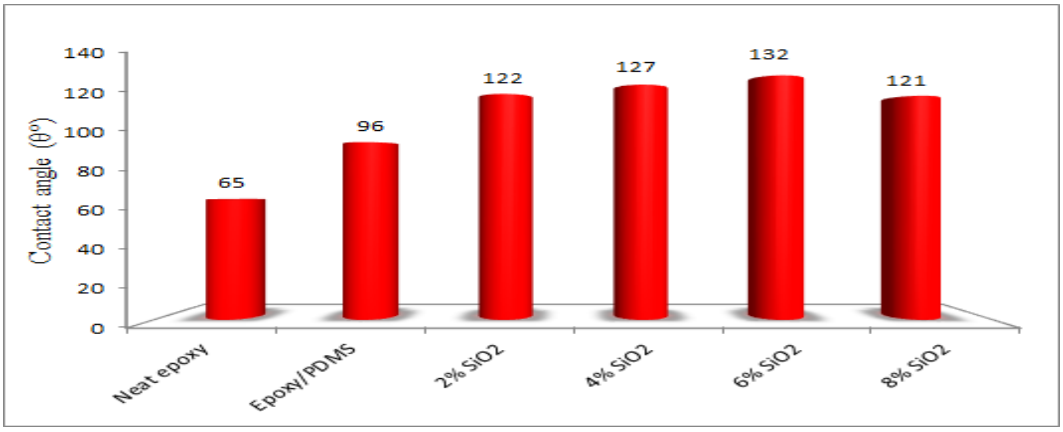

Figure 4.5: The effect of SiO_2 nanoparticles on the contact angle values

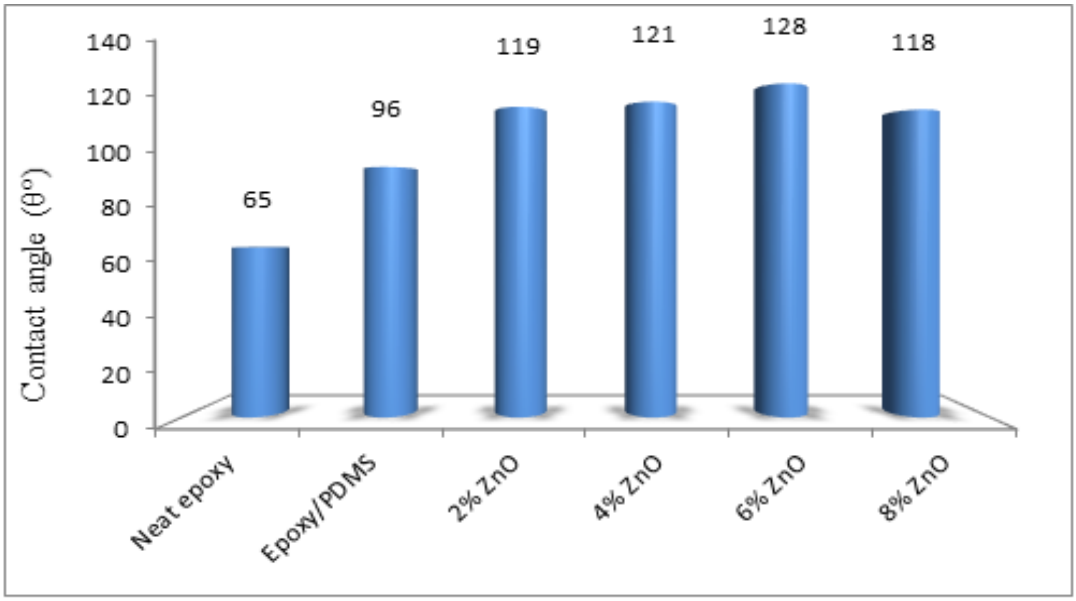

Figure 4.6: The effect of ZnO nanoparticles on the contact angle values

4.4 Surface morphology

Visual observation could not reveal the surface morphology of the coatings and how well the nanoparticles disperse within the polymeric matrix. For this reason, Field Emission Scanning Electron Microscopy (FESEM) was used to investigate the dispersion state of the nanoparticles and its effect on the surface roughness of the developed coating systems.

The surface microstructure, as well as the roughness and the surface free energy, are considered as the most effective factors on the wettability of the coating surface (T. Bharathidasan et al., 2014). Figure 4.7. (a) and (b) show FESEM micrographs of neat epoxy and silicone modified epoxy coating system

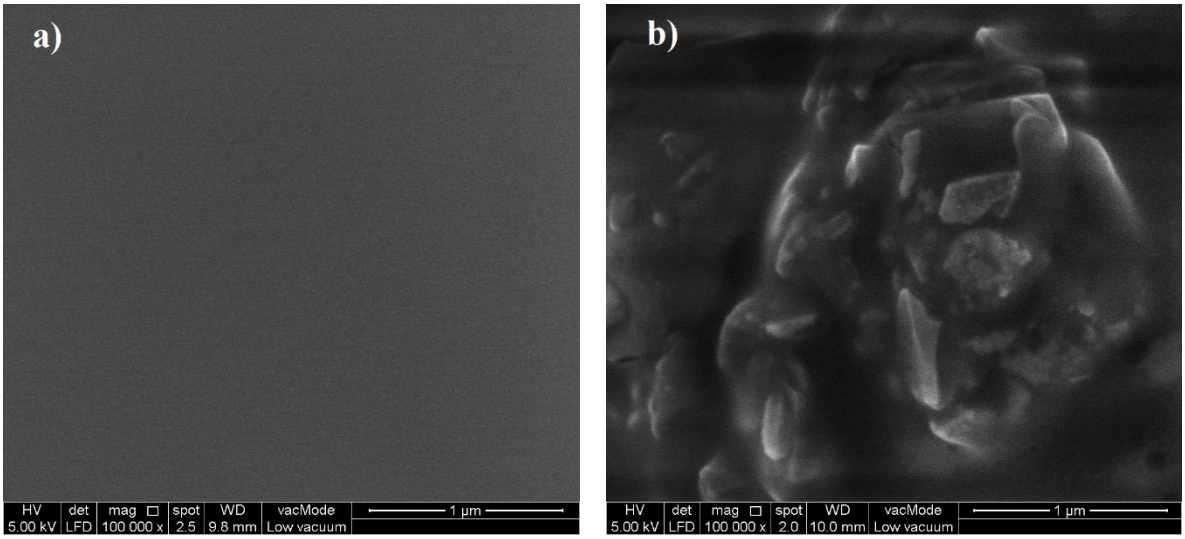

Figure 4.7: FESEM micrographs of (a) neat epoxy and (b) silicone modified epoxy coatings

The FESEM image of unmodified epoxy coatings (Figure 4.7.a) reveals smooth surface which is in complete agreement with the hydrophilicity nature observed in the contact angle measurement. Heterogeneous morphology with increasing in the surface roughness were observed in the image of silicone modified epoxy sample as shown in Figure. 4.7 (b). This observation confirms the existence of inter crosslinking structure in epoxy modified with PDMS system (Ananda Kumar & Sankara Narayanan, 2002).

The effect of SiO_2 nanoparticles on enhancing the hydrophobicity of the surface was clearly confirmed in FESEM micrographs as depicted in Figure.4.8 (a)-(d). As the content of the nanoparticles increased, the roughness of the surface increased. Uniform distribution of nanoparticles particularly at 6 wt.% SiO_2 nanoparticles increases the roughness with corresponding 132° of water contact angle. Improving the hydrophobicity result from the incorporation of SiO_2 nanoparticles with the PDMS-epoxy matrix could be attributed to the

ability of the rough surface to form air pockets between water and the surface leading to composite solid-liquid-air interface (Bharathidasan et al., 2014).

In the case of using ZnO nanoparticles to reinforce silicone modified epoxy matrix. The same effect of SiO_2 nano fillers was observed with ZnO. The roughness of the coating surface increased with a further addition of ZnO nanoparticles. The micrographs were in complete agreement with the results of contact angle measurements. 6% weight loading of ZnO nano fillers shows good compatibility with the PDMS-epoxy matrix with recorded water contact angle up to 128°. Figure 4.9 shows the FESEM image of ZnO nanocomposites at various loading rates.

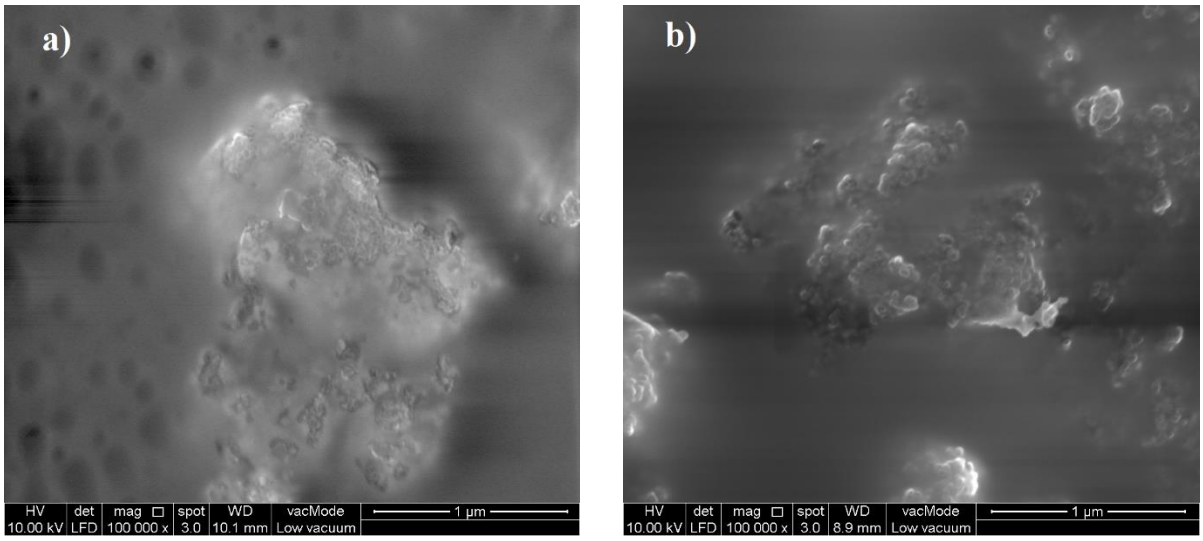

Figure 4.8: FESEM micrographs of SiO_2 nanocomposites with (a) 2, (b) 4, 6 and 8 wt.% SiO_2 nanoparticles

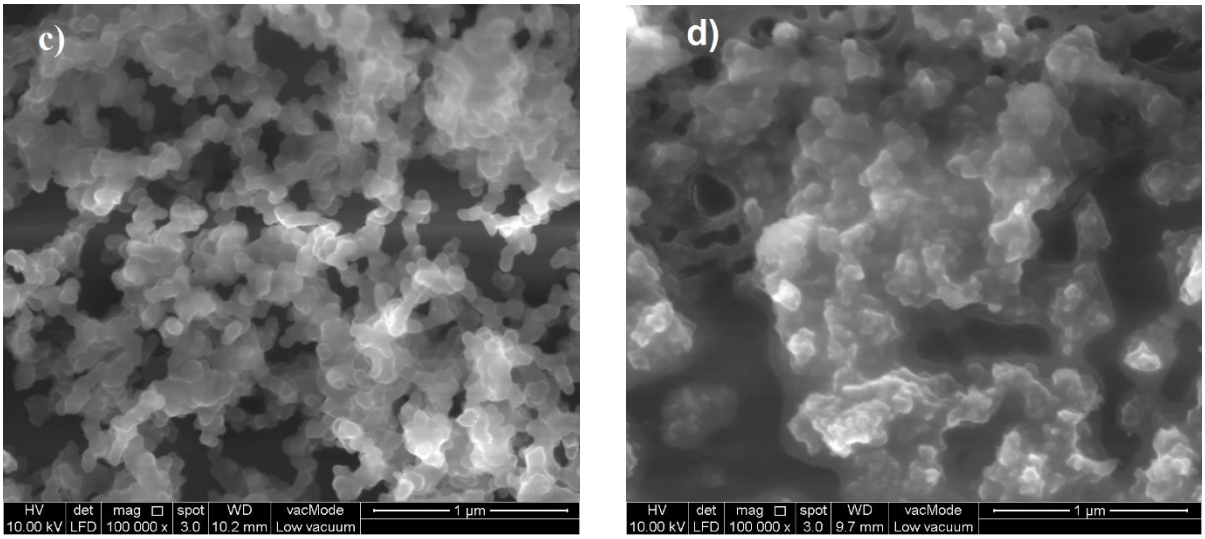

Figure 4.8: continued

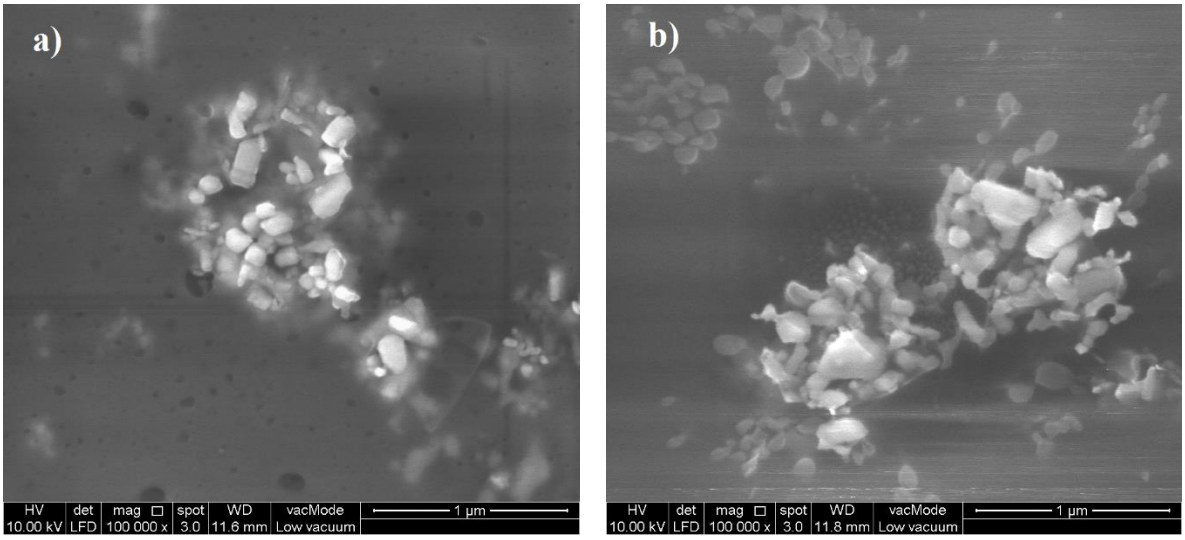

Figure 4.9: FESEM micrographs of ZnO nanocomposites with (a) 2, (b) 4, 6 and 8 wt.% ZnO nanoparticles

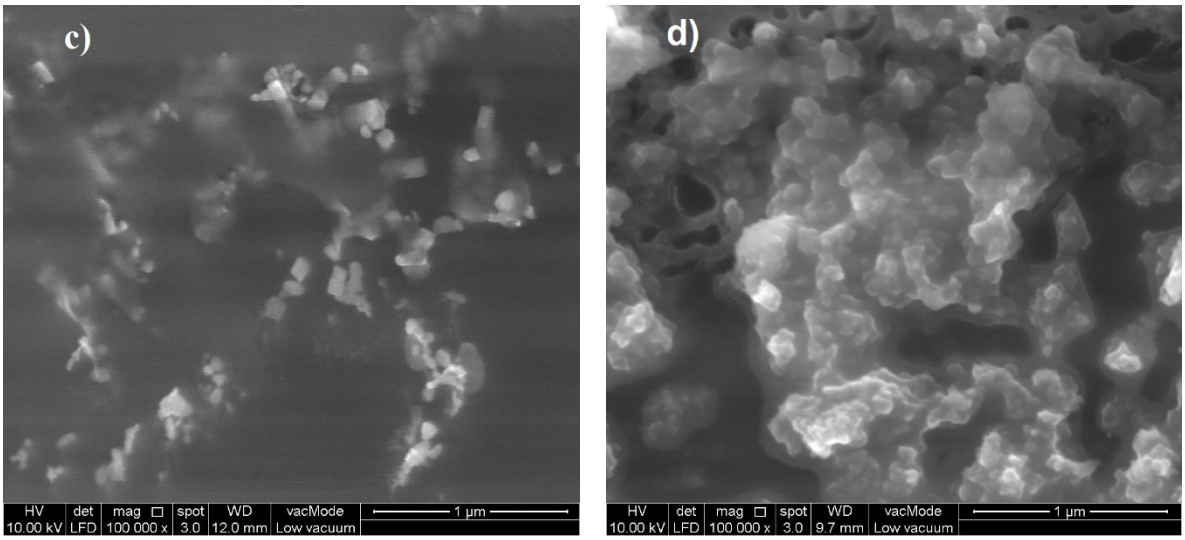

Figure 4.9: continued

4.5 Electrochemical impedance spectroscopy (EIS)

In this study, EIS data in the form of Bode and Nyquist plots were used to determine the coating resistance (R_c) and coating capacitance (C_c) of the prepared samples. EIS considers as a powerful technique to investigate the adhesion characteristics of the coatings to the substrate. In addition, capacitance measurements help in estimating the uptake rates of the electrolyte by the coating films and can be used to evaluate the delamination rates of the coating from the substrate surface.

In terms of obtaining the resistance, capacitance, water uptake and dielectric constant of the developed coatings, the electrical equivalent circuits illustrated in Figure 4.10 were utilized to describe the behavior of the coated panels before and after the electrolyte reaching to the metallic substrate and to fit the data obtained from EIS measurements. This circuits consist of R_s which represent the electrolyte's uncompensated resistance between the working and reference electrodes, the coating resistance R_c which in terms result from the

electrolyte penetration into the coating's micro pores, C_c is the coating capacitance, C_d represents the double layer capacitance and the polarization resistance of the substrate working electrode is given by R_p. For all EIS data, the equivalent circuits mentioned above was used to fit the obtained results by the assist of Echem Analyst Version 6.03 software.

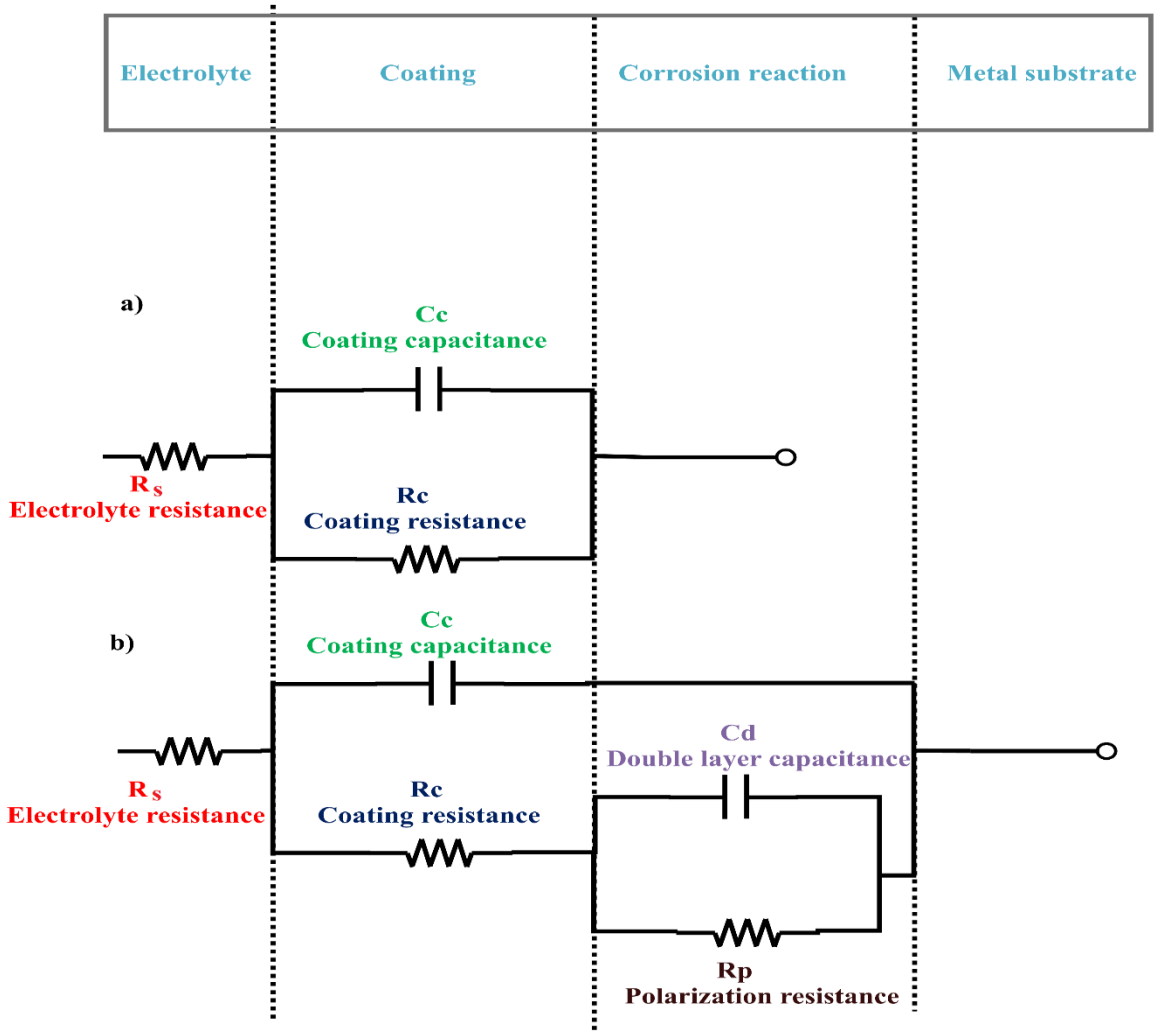

Figure. 4.10: Equivalent circuits used for the fitting of impedance plots (Nematollahi et al., 2010). (a) Before electrolyte reaches the substrate surface and (b) after initiation of corrosion due to electrolyte penetration

4.5.1 Evaluation of the anti-corrosion performance of the developed coatings

4.5.1.1 Silicone modified epoxy coating system

The Bode and Nyquist plots of unmodified epoxy and silicone modified epoxy systems after 1, 15 and 30 days of immersion time in 3% NaCl solution at their corresponding open circuit potential are shown in Figures. 4.11- 4.13. From Figures 4.11 (a) and (b) it is found that the coating resistance value for the neat epoxy was found to be in the range of $10^9\Omega$ after 24h of immersion. An increase in the coating resistance (R_c) was observed after the incorporation of polydimethylsiloxane with the epoxy resin. Coating resistance of $10^{10}\ \Omega$ was noted for PDMS-epoxy mixture for the same period of immersion. That can be explained as the barrier performance of both coatings against the corrosive electrolyte diffusion after 1 day. The coating resistance of the unmodified epoxy decreased significantly after 15 days of immersion. The results show that coating resistance ($< 10^6\ \Omega$) was recorded for epoxy coating with two semicircles, in Nyquist plot, which corresponded to two capacitive time constant. That in turn can be attributed to the coating degradation due to the electrolyte diffusion (E. Matin et al., 2015). On the contrary, PDMS modified epoxy coating system shows no significant change in the shape and or the slope of Bode plot as well as the diagram in Nyquist plot after 15 days of immersion. The most pronounced decrease of the PDMS-epoxy coating resistance was after 30 days of immersion where $R_c = 10^8\ \Omega$ was recorded.

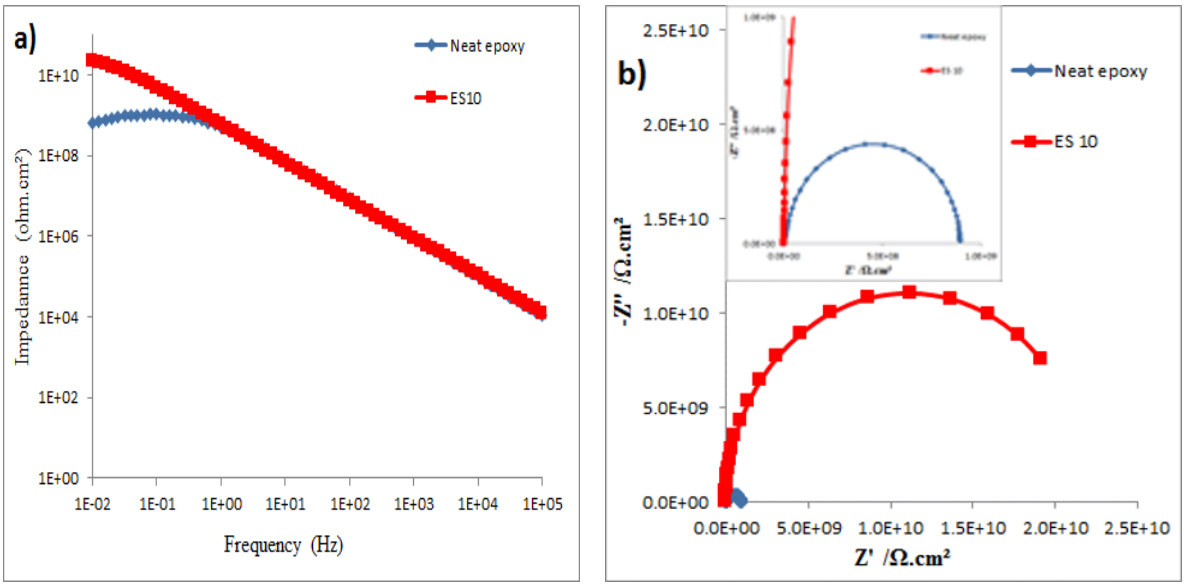

Figure 4.11: Representative (a) Bode and (b) Nyquist plots of neat epoxy and PDMS-epoxy (ES10) coating systems after 1 day of immersion

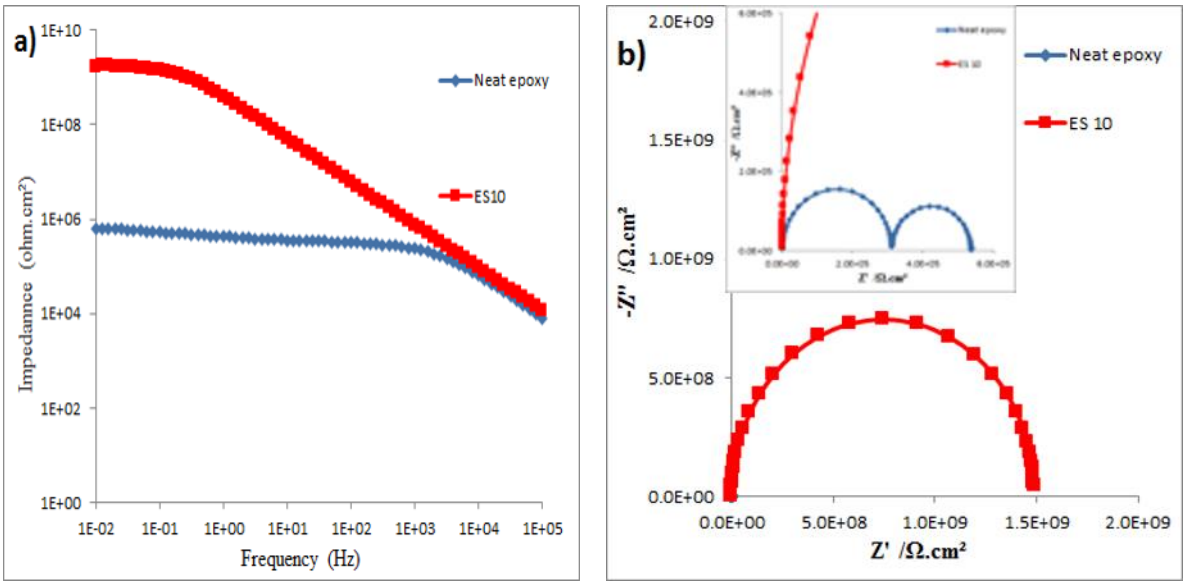

Figure 4.12: Representative (a) Bode and (b) Nyquist plots of neat epoxy and PDMS-epoxy (ES10) coating systems after 15 days of immersion

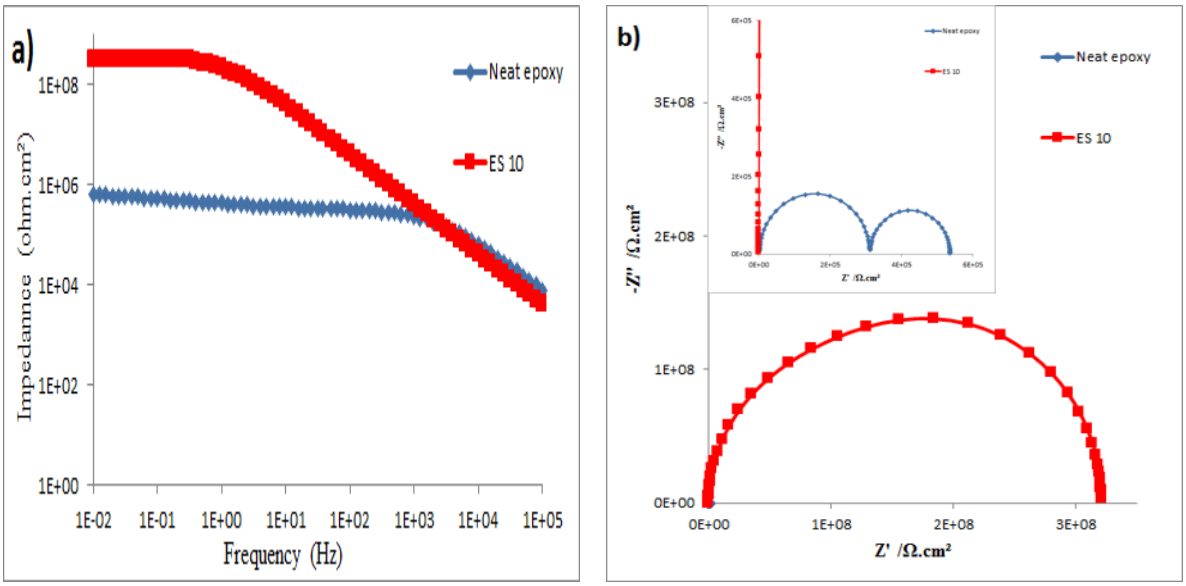

Figure 4.13: Representative (a) Bode and (b) Nyquist plots of neat epoxy and PDMS-epoxy (ES10) coating systems after 30 days of immersion

S. Ananda Kumar et al., (2002) have explicated the enhancement of the corrosion resistant of the steel surface coated with the siliconized epoxy interpenetrating coatings over the conventional coatings by the lower permeability of the coatings contain PDMS and its ability to limiting the corrosion of the substrate by a diffusion barrier type mechanism.

4.5.1.2 SiO_2 nanocomposite coating

In order to monitor and predict the anti-corrosion performance of the developed hybrid organic-inorganic nanocomposite coatings reinforced with SiO_2 nano fillers, Bode and Nyquist plots after 1, 15 and 30 days of immersion, as shown in Figures 4.14 – 4.16, were analyzed. All recorded results show a straight line in the Bode plot with a slope of -1

which indicates that coatings at all nanoparticles loading rates obtained superior barrier behavior after 24 h of exposure to 3% NaCl solution. High coating resistance (R_c) values in the range of 10^{11} Ω were recorded. As the days progressed, the system with 2% weight percentage of nano SiO_2 remains having the same value of resistance at approximately 10^{11} Ω. This performance was also observed even up to 30 days of immersion, indicating that the addition of a small amount of silica dioxide nanoparticles, 2 wt.% , has a huge influence on the anti-corrosion performance during all the experiment time without any sign of corrosion start. This super corrosion protection can be attributed to the important role that the nano SiO_2 particles play in forming an efficient physical barrier against water and corrosive agents toward the coating/substrate interface and in zigzagging the pathways which in turn enforce the corroding agents to travel a longer tortuous path to reach the surface of the substrate (E. Matin et al., 2015; Nematollahi et al., 2010; L. Sun et al., 2008).

However, the other loading rates of nano SiO_2 fillers had a good effect on the corrosion protection properties of the coatings during the first 15 days of the immersion period. A slight enhancement in the coating resistance with the addition of 4 wt.% and 6 wt.% of SiO_2 was observed up to 30 days. While, on the contrary, 8 wt.% of nano SiO_2 within the PDMS-epoxy matrix shows a lower enhancement on the barrier performance where R_c value less than 10^8 Ω was recorded. That in turns can be explained due to the trend of the nanoparticles to form agglomerations at high loading rates (Ramezanzadeh et al., 2011). Figure 4.17 shows the relation between the coating resistance and the SiO_2 nanoparticles content at different immersion time in 3% NaCl.

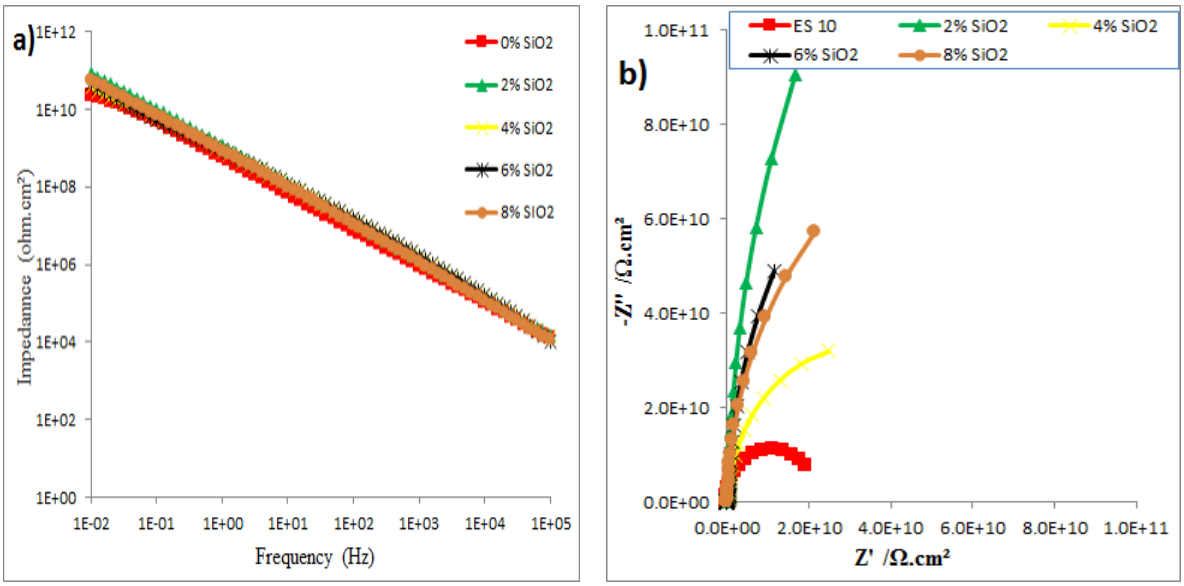

Figure.4.14: Representative (a) Bode and (b) Nyquist plots of 0, 2, 4, 6 and 8 wt.% of SiO_2 nanocomposite coating systems after 1 day of immersion

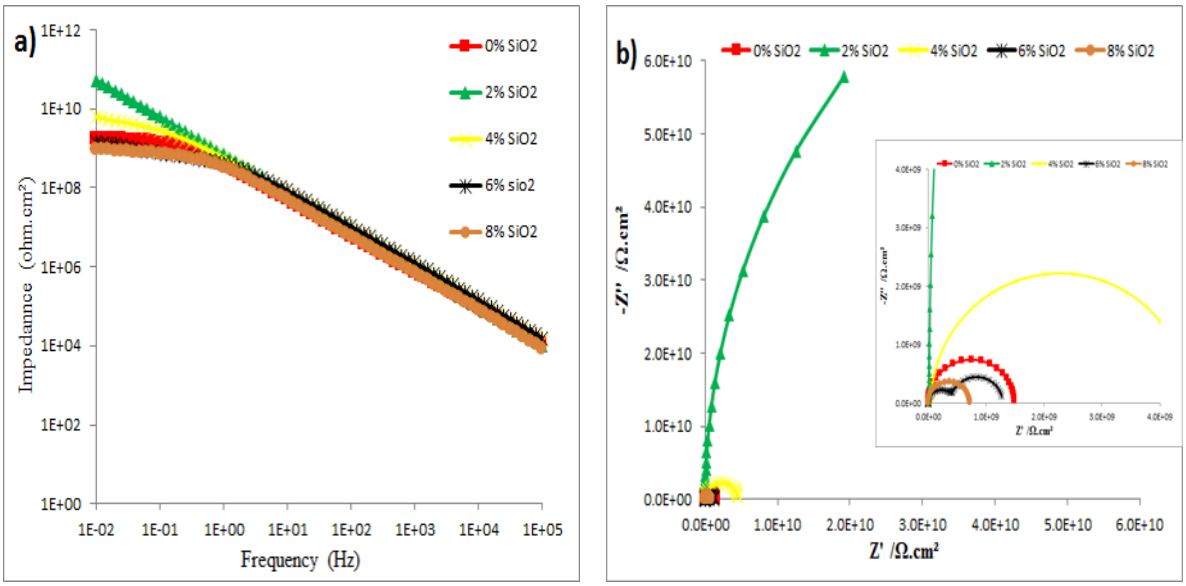

Figure.4.15: Representative (a) Bode and (b) Nyquist plots of 0, 2, 4, 6 and 8 wt.% of SiO_2 nanocomposite coating systems after 15 days of immersion

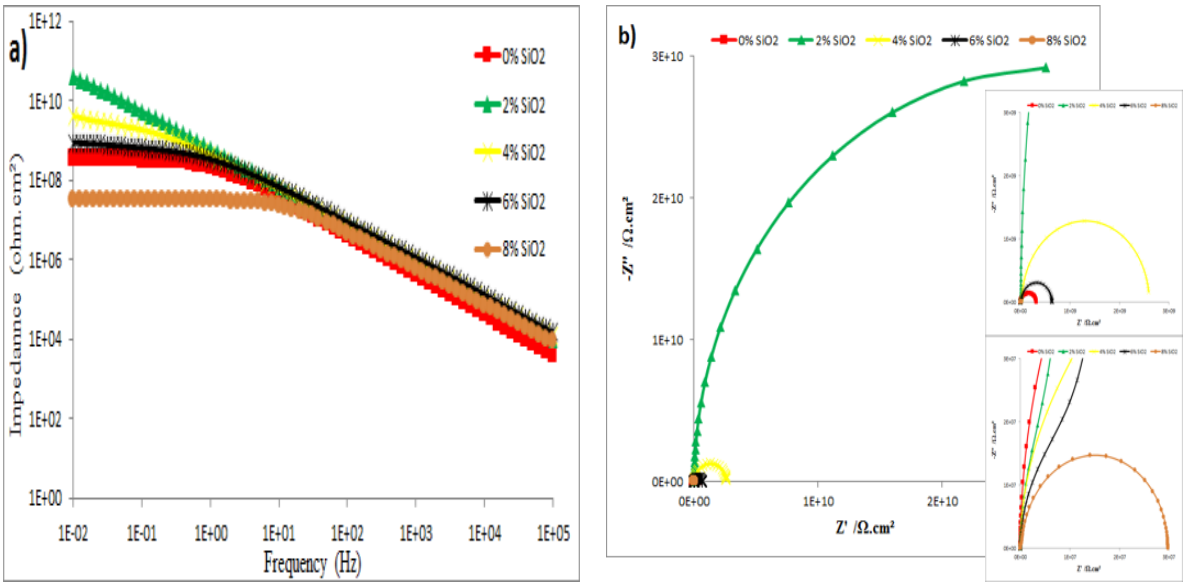

Figure.4.16: Representative (a) Bode and (b) Nyquist plots of 0, 2, 4, 6 and 8 wt.% of SiO_2 nanocomposite coating systems after 30 days of immersion

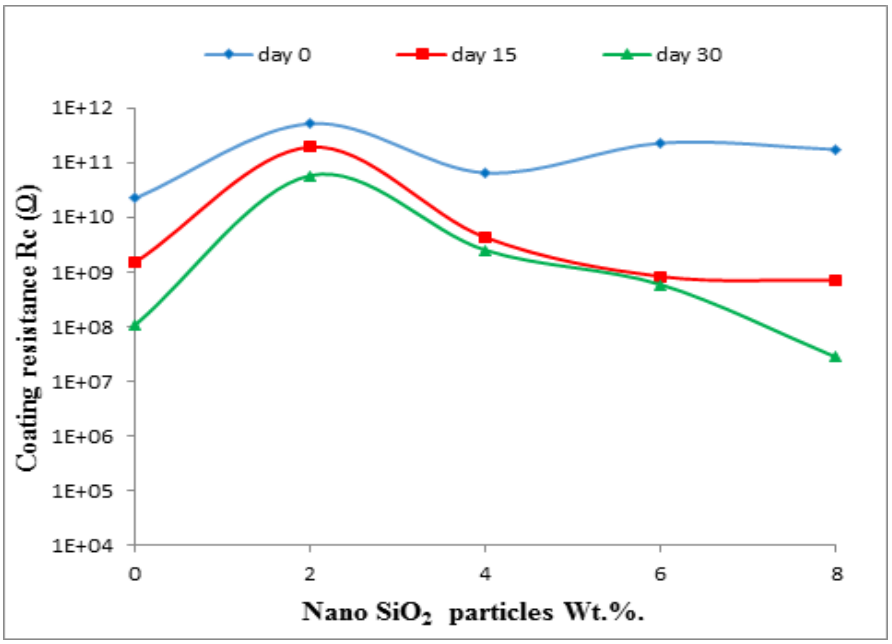

Figure 4.17: The influence of SiO_2 nanoparticles content in enhancing the coating resistance during the immersion time.

4.5.1.3 ZnO nanocomposite coating

The data obtained from EIS measurements after 1, 15 and 30 days, as time of exposure to 3% NaCl solution, are shown in Figures 4.18 – 4.20. The impedance plots after different immersion periods were fitted by using the electrical equivalent circuits illustrated in Figure 4.10. Extremely high resistance (R_c) for all prepared coatings was observed after 24 h of immersion Figure 4.18.a. In addition, observation of a straight line in the Bode plot with a slope of -1 was noted which in turn indicates a capacitive behavior of the coatings. The addition of ZnO particles results in superior anti-corrosion performance as the coating resistance improved up to 1 x 10^{11} Ω.

After 15 days of immersion, the impedance value obtained from EIS spectra of the specimen with 2 wt.% nano ZnO shows no significant change in the shape and or the slope of Bode plot as well as the diagram in Nyquist plot. That in turn confirms the ability of the low loading ratio of nano-sized particles of zinc oxide to enhance the barrier performance of the coating against electrolyte penetrating up to 15 days. No further increase in the corrosion resistance was results from the addition of 4, 6 or 8 wt.% of ZnO nanoparticles. But, on the contrary, the impedance decreased significantly, with the increase in immersion time, when 6 wt.% and more pronounced at 8 wt.% ZnO was utilized.

As the days progressed, superior corrosion protection was clearly observed for the system with 2 wt.% at R_c > 10 GΩ cm^2 up to 30 days of immersion. This obviously shows that ZnO nano fillers have the capability to enhance the corrosion protection, of the silicone modified epoxy matrix, significantly with excellent barrier performance.

Ramezanzadeh et al., (2011b) and Shi et al., (2009) have suggested that, the overall corrosion protection performance of the organic coatings, based on epoxy resin, can be enhanced by the incorporation of ZnO nanoparticles through the following main mechanisms: First, well-dispersed ZnO nanoparticles within the polymeric matrix lead to enhancing the quality of the coating film by reducing the porosity and zigzagging the diffusion pathways which in turn result in improving the barrier properties of the coating. Second, the employment of the ZnO nanoparticles increases the adherence of the cured epoxy to the surface of the substrate. Furthermore, the physical nature of the interactions between the nano-sized ZnO particles and the polymeric matrix, compared to the chemical interaction among the resin chains, consider more efficient in improving the resistance against the hydrolytic degradation.

However, the other nanocomposite systems perform a decreasing in the corrosion resistance. It is worth to be mentioned that the values of the nanocomposite systems, especially for using of 4 wt.% ZnO nanoparticles, are considerably higher than that related to the neat epoxy after the same period of immersion. Lower corrosion resistance of the coatings reinforced with 4,6 and 8 wt.% comparing to the system loaded with 2 wt.% ZnO can be explained as follows: as the amount of the nanoparticles increase within the polymeric matrix, the cross-linking density decrease. Furthermore, high tendency of the nanoparticles to form aggregations at high loadings, especially at 8 wt.%, can lead to a reducing in the barrier performance of the coatings (Ramezanzadeh et al., 2011b). Figure 4.21 shows the relation between the coating resistance and the ZnO nanoparticles content at different immersion time in 3% NaCl.

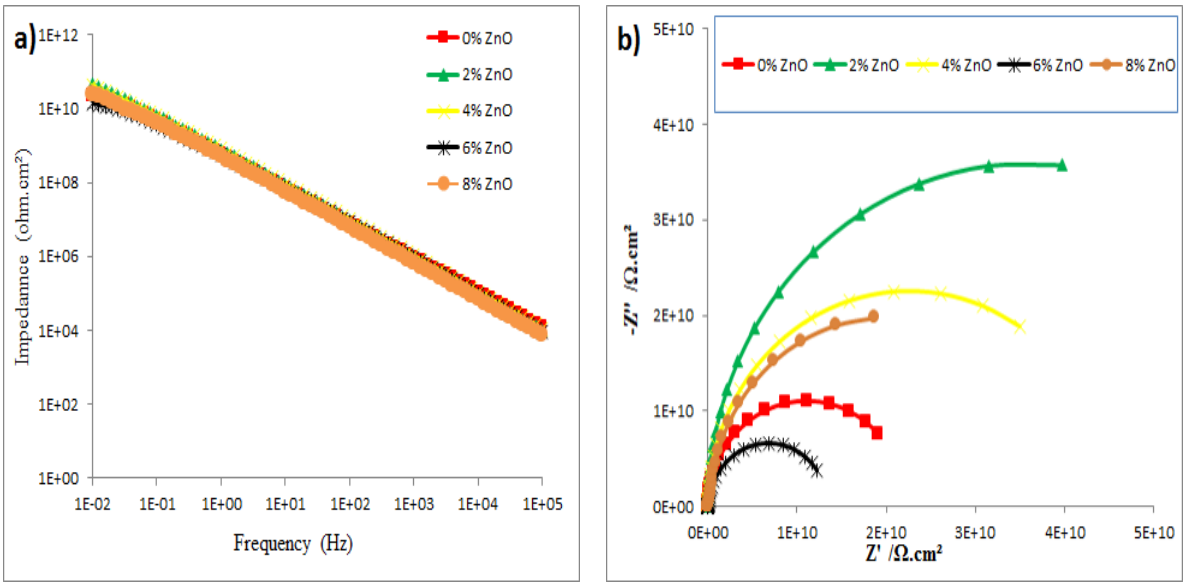

Figure.4.18: Representative (a) Bode and (b) Nyquist plots of 0, 2, 4, 6 and 8 wt.% of ZnO nanocomposite coating systems after 1 day of immersion

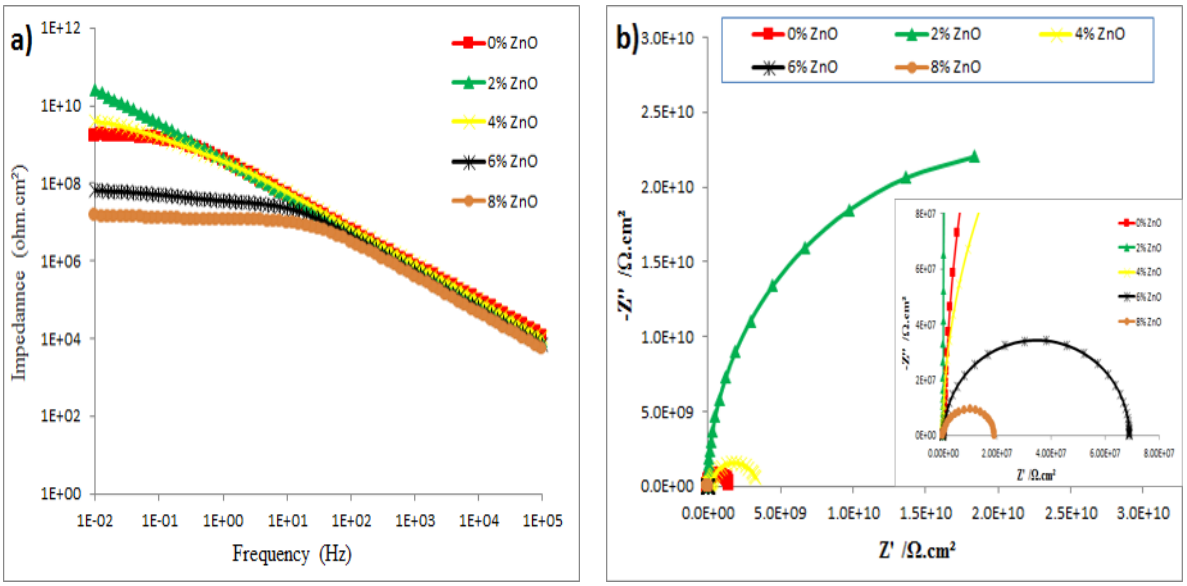

Figure.4.19: Representative (a) Bode and (b) Nyquist plots of 0, 2, 4, 6 and 8 wt.% of ZnO nanocomposite coating systems after 15 days of immersion

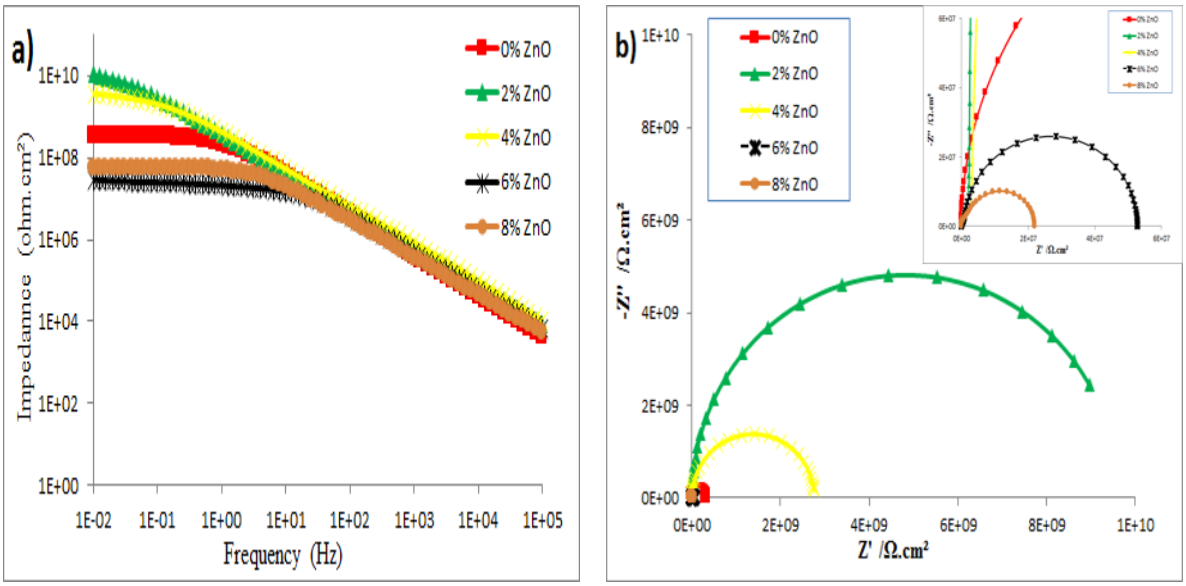

Figure.4.20: Representative (a) Bode and (b) Nyquist plots of 0, 2, 4, 6 and 8 wt.% of ZnO nanocomposite coating systems after 30 days of immersion

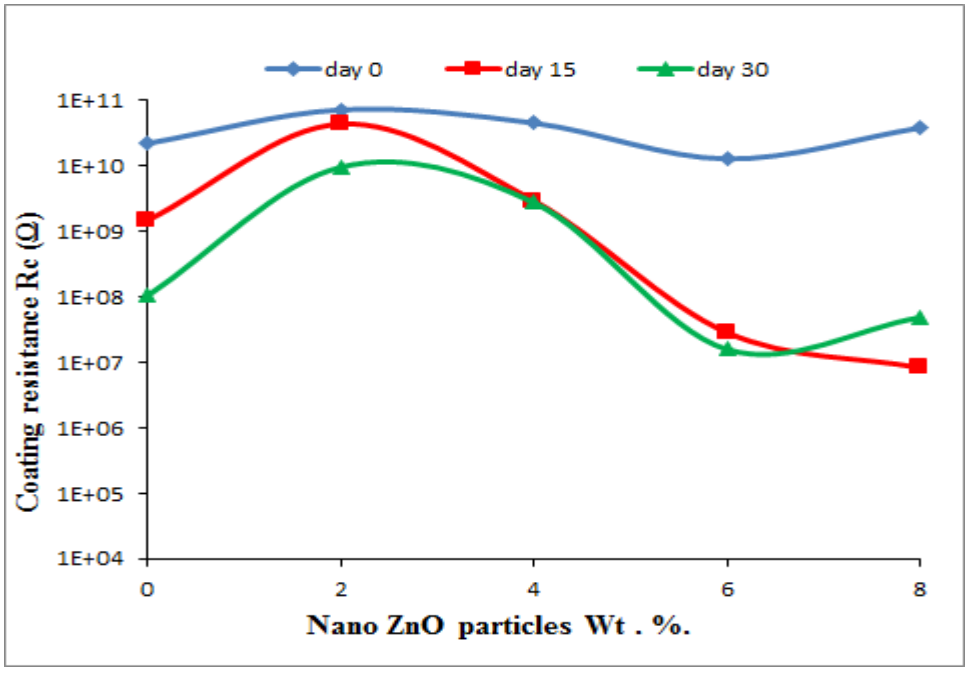

Figure 4.21: The influence of ZnO nanoparticles content in enhancing the coating resistance during the immersion time.

Figure 4.22 illustrates the coating capacitance (C_c) of SiO_2 and ZnO nanocomposite coatings, which is related the exposed area of the sample to the electrolyte. The value of the C_c increases as the days progressed due to the increment in the loss of adhesion between the coating film and the substrate.

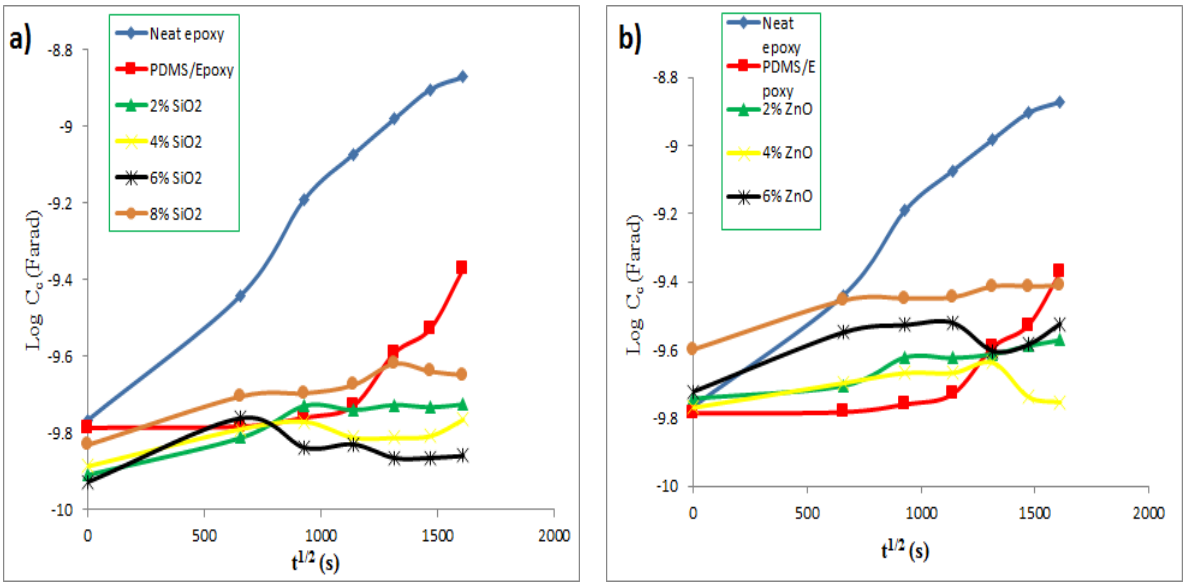

Figure 4.22: Coating capacitance (Cc) vs. Time of immersion for (a) SiO_2 nanocomposite coating systems and (b) ZnO nanocomposite coating systems

The results of the nano composites reinforced with SiO_2 nano fillers show that there are no significant differences between the C_c values of all addition rates of nanoparticles with low values in the range of 10^{-10} Farad. Ramesh et al., (2013) have reported that the high-performance coatings show low coating capacitance values. For the using of ZnO nanoparticles within the PDMS-epoxy matrix, the same behavior of the coating films up to 30 days of exposure time was observed with low C_c values in the range of 10^{-10} Farad for all ZnO loading rates.

Ramesh et al., (2013) and Rau et al., (2012) have used capacitance measurements to determine the water uptake in organic coatings. Figures. 4.23 and 4.24 present the dielectric constant and water uptake, respectively of PDMS-epoxy hybrid nanocomposite coatings during 30 days of immersion in 3% NaCl solution.

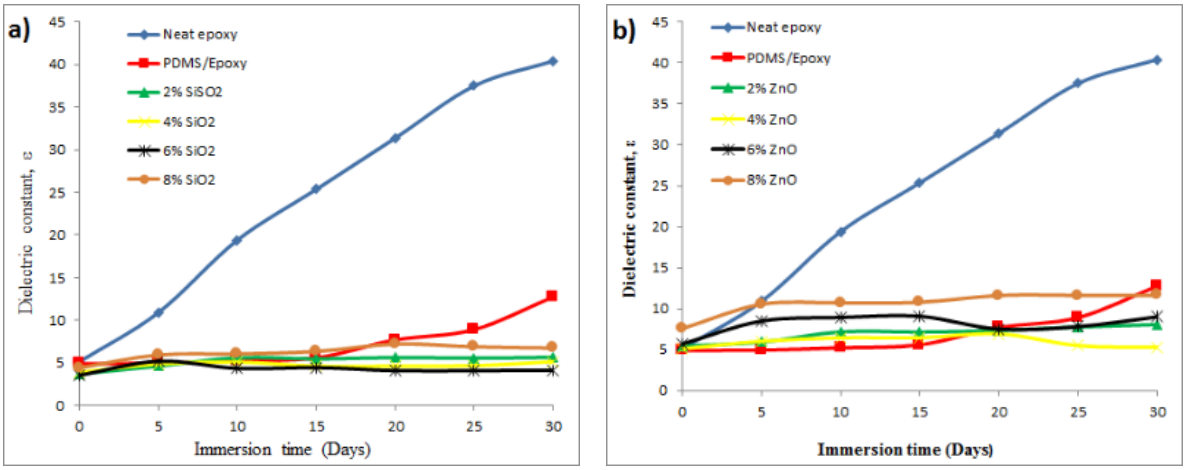

Figure 4.23: Dielectric constant (ε) vs. Time of immersion for a) SiO_2 nanocomposite coating systems and b) ZnO nanocomposite coating systems

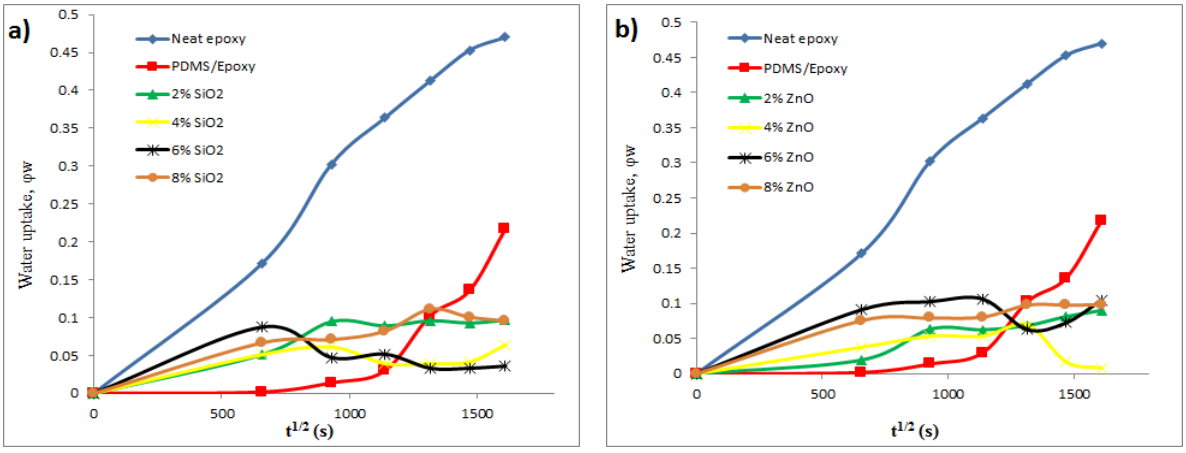

Figure 4.24: Water uptake (φ_w) vs. Time of immersion for a) SiO_2 nanocomposite coating systems and b) ZnO nanocomposite coating systems

The method to obtain the amount of water absorbed by the coating film from the capacitance data is well described by (Amirudin & Thierry, 1995; Rau et al., 2012) as follows:

$$C = (\varepsilon . \varepsilon_0 . A)/d \qquad \text{(I)}$$

Where:

C: the capacitance of the coating (F).

ε: dielectric constant

ε_0: dielectric constant of free space (8.85×10^{-12} F/m)

A: the surface area of the exposed coating (m^2)

d: the coating thickness (m)

The solid, water, and air tri phase coating has dielectric constant as reported by (Castela & Simoes, 2003) as follows:

$$\varepsilon = \varepsilon_s . \varepsilon_w . \varepsilon_a \qquad \text{(II)}$$

Where ε_s, ε_w ($\approx$80), and ε_a ($\approx$ 1) are the dielectric constant of solid, water and air-mixed respectively. By analyzing the data of the dielectric constant of the SiO_2 nanocomposite coatings, it is quite clear that all systems reinforced with the nano fillers exhibits small porosity and possesses good barrier properties. Likewise, the results of ZnO nano composites show the same effect of incorporation of the inorganic nanoparticles within

the polymeric matrix. The presence of pores and voids was related to unmodified epoxy and PDMS-epoxy coating due to the increase that occurs to the dielectric constant values comparing to the nanocomposite coatings. Electrolyte uptake and transport of ions (Na^+ and Cl^-) at the coating/metal interface could be results from the existence of the pores and voids mentioned above (Rau et al., 2012).

For the calculation of the water uptake value the following equation was used (Amirudin & Thierry, 1995; Castela & Simoes, 2003):

$$\varphi_W = \frac{log(\frac{C_t}{C_0})}{log\varepsilon_w}$$

Where C_t is the capacitance at time t of immersion and C_o is the capacitance at t=0. When φ_w increases, ε_W increases, resulting in higher capacitance. While, the impedance of the coatings systems was high for all loadings rate of nanoparticles either the SiO_2 or ZnO type. The capacitance was found to be low which is comforting the barrier performance of the coating films. As a result of that the water uptake and the dielectric constant were also found with no significant difference between the coating systems. However, in the case of utilizing SiO_2 nano fillers, the most pronounced increment in the water uptake value up to 30 days of exposure was related to the use of 8 wt.% nano SiO_2. That effect was also observed for the same loading ratio of ZnO nanoparticles.

The values of the coating resistance, the capacitance, the dielectric constant and the water uptake of the two developed nanocomposite systems are tabulated in Tables 4.3 - 4.6.

Table 4.3: Coating resistance and coating capacitance values after 1, 15 and 30 days of immersion in 3% NaCl of neat epoxy, silicone modified epoxy and SiO_2 nanocomposite coating system

System / Day	Coating resistance R_c (Ω)			Coating capacitance C_c (Farad)		
	1	15	30	1	15	30
Neat epoxy	7.5×10^{8}	5.6×10^{5}	8.4×10^{4}	2.0×10^{-10}	8.0×10^{-10}	1.0×10^{-9}
PDMS/ epoxy	2.2×10^{10}	1.5×10^{9}	1.0×10^{8}	1.4×10^{-10}	2.5×10^{-10}	5.0×10^{-10}
2% SiO_2	5.2×10^{11}	1.9×10^{11}	5.8×10^{10}	1.2×10^{-10}	1.3×10^{-10}	1.4×10^{-10}
4% SiO_2	6.5×10^{10}	4.3×10^{9}	2.5×10^{9}	1.2×10^{-10}	1.8×10^{-10}	1.7×10^{-10}
6% SiO_2	2.3×10^{11}	8.3×10^{8}	5.8×10^{8}	1.2×10^{-10}	1.5×10^{-10}	2.9×10^{-10}
8% SiO_2	1.7×10^{11}	7.1×10^{8}	2.7×10^{7}	1.2×10^{-10}	2.6×10^{-10}	6.0×10^{-10}

Table 4.4: Dielectric constant and water uptake values after 1, 15 and 30 days of immersion in 3% NaCl of neat epoxy, silicone modified epoxy and SiO_2 nanocomposite coating system

System / Day	Dielectric constant, ε			water uptake, φ_w		
	1	15	30	1	15	30
Neat epoxy	5	25	40	0.1	0.3	0.45
PDMS/ epoxy	5	8	12	0.001	0.02	0.2
2% SiO_2	3	5	5	0.0001	0.005	0.08
4% SiO_2	3	5	6	0.0002	0.008	0.05
6% SiO_2	3	4	5	0.0001	0.009	0.04
8% SiO_2	4	5	6	0.0001	0.06	0.1

Table 4.5: Coating resistance and coating capacitance values after 1, 15 and 30 days of immersion in 3% NaCl of neat epoxy, silicone modified epoxy and ZnO nanocomposite coating system

System / Day	Coating resistance R_c (Ω)			Coating capacitance C_c (Farad)		
	1	15	30	1	15	30
Neat epoxy	7.5×10^{8}	5.6×10^{5}	8.4×10^{4}	2.0×10^{-10}	8.0×10^{-10}	1.0×10^{-9}
PDMS/ epoxy	2.2×10^{10}	1.5×10^{9}	1.0×10^{8}	1.4×10^{-10}	2.5×10^{-10}	5.0×10^{-10}
2% ZnO	7.2×10^{10}	4.4×10^{10}	9.6×10^{9}	1.8×10^{-10}	2.3×10^{-10}	2.6×10^{-10}
4% ZnO	4.5×10^{10}	2.9×10^{9}	2.7×10^{9}	1.7×10^{-10}	2.5×10^{-10}	2.2×10^{-10}
6% ZnO	1.2×10^{10}	1.6×10^{8}	2.8×10^{7}	1.9×10^{-10}	2.7×10^{-10}	3.2×10^{-10}
8% ZnO	3.8×10^{10}	4.8×10^{7}	1.5×10^{7}	1.2×10^{-10}	2.6×10^{-10}	5.8×10^{-10}

Table 4.6: Dielectric constant and water uptake values after 1, 15 and 30 days of immersion in 3% NaCl of neat epoxy, silicone modified epoxy and ZnO nanocomposite coating system

System / Day	Dielectric constant, ε			water uptake, φ_w		
	1	15	30	1	15	30
Neat epoxy	5	25	40	0.1	0.3	0.45
PDMS/ epoxy	5	8	12	0.001	0.02	0.2
2% ZnO	5	7	8	0.002	0.06	0.07
4% ZnO	5	6	7	0.001	0.04	0.05
6% ZnO	5	8	9	0.001	0.06	0.09
8% ZnO	7	10	11	0.07	0.08	0.1

4.6 Differential Scanning Calorimetry (DSC) Analysis

Investigating the thermal properties of the developed coatings and the changes that took place according to absorbing heat energy by the samples were carried out by using Differential Scanning Calorimetry (DSC) technique. All prepared samples, which include neat epoxy, epoxy modified with PDMS and two types of nanoparticles reinforced samples, were tested by DSC.

Glass transition temperature (T_g) of the blend changes with chemical constitution, tacticity, molecular weight, amount and nature of pigments and reinforcement additives, morphology of the binder, the presence or absence of plasticizers and the degree of cross-linking. Therefore, T_g is widely accepted as a predominant factor in determining the physical and mechanical properties of a coating system. DSC curves of neat epoxy and epoxy modified with PDMS are illustrated in Figure 4.25. While the DSC results for SiO_2 and ZnO nanocomposite samples are shown in Figures 4.26 and 4.27 respectively. Glass transition temperatures (T_g) values of all prepared systems were tabulated in Tables 4.7 and 4.8. Single glass transition temperature was observed in all DSC thermograms which can be related to the presence of inter-cross linked network structure as reported by (Ananda Kumar & Sankara Narayanan, 2002).

Table 4.7: Glass transition temperature of neat epoxy, PDMS-epoxy and SiO_2 nanocomposite coating systems

System	Glass transition temperature, T_g (°C)
Neat epoxy	85.9
PDMS/ epoxy	93.0
2% SiO_2	95.0
4% SiO_2	86.3
6% SiO_2	80.7
8% SiO_2	74.8

Table 4.8: Glass transition temperature of neat epoxy, PDMS/epoxy and ZnO nanocomposite coating systems

System	Glass transition temperature T_g (°C)
Neat epoxy	85.9
PDMS/ epoxy	93.0
2% ZnO	84.0
4% ZnO	82.3
6% ZnO	80.0
8% ZnO	77.4

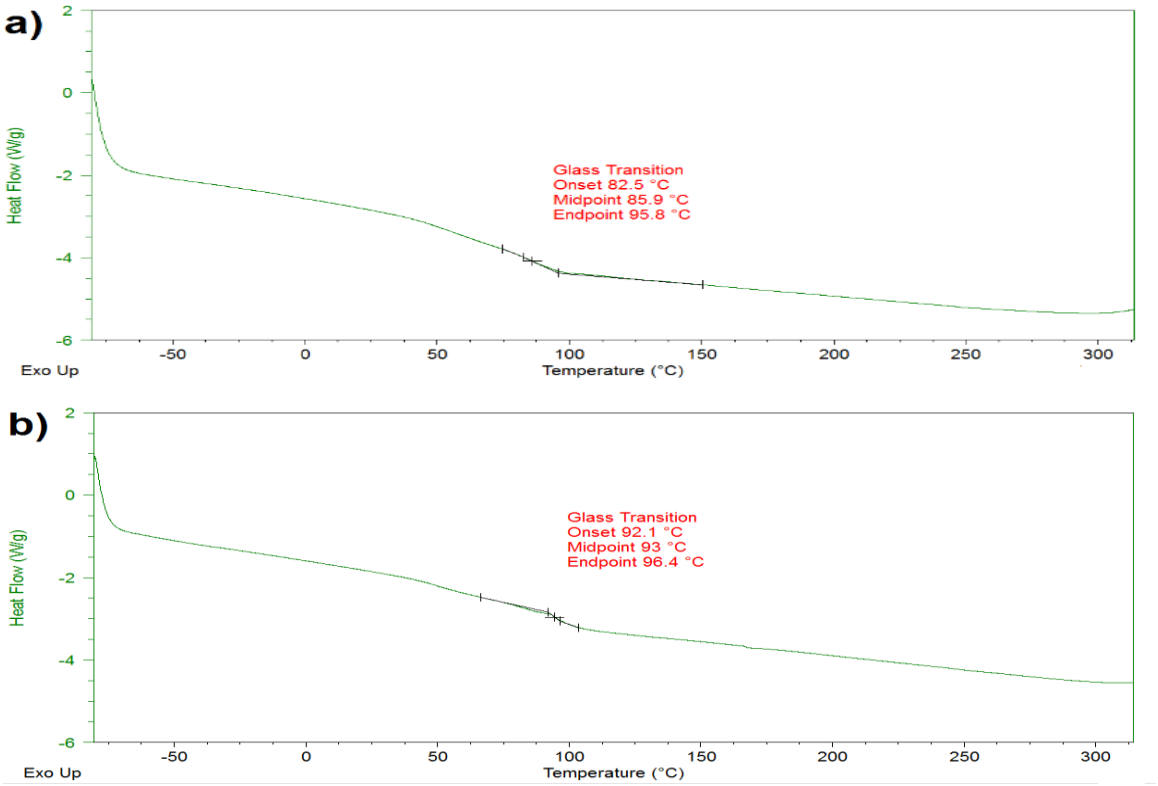

Figure 4.25: DSC curves of (a) neat epoxy and (b) PDMS-epoxy coating systems

By inspecting the data that tabulated in Table 4.5, it can be understood that the incorporation of PDMS with the epoxy resin increases the glass transition temperature of the blend. It can be observed that the T_g of neat epoxy was found to be 86 °C. Whereas, the incorporation of 10 wt.% PDMS with the epoxy resin result in an improvement in the T_g of the binder to become equal to almost 93 °C. Velan & Bilal, (2000) have reported that by the increment of the polydimethylsiloxane content within the siliconized epoxy interpenetrating network, an additional increment in the T_g could be observed. It is predicted that the incorporation of silicone enhances the cross-linking of epoxy resin which in turn leads to low free volume concentration as the molecules close up during the curing process.

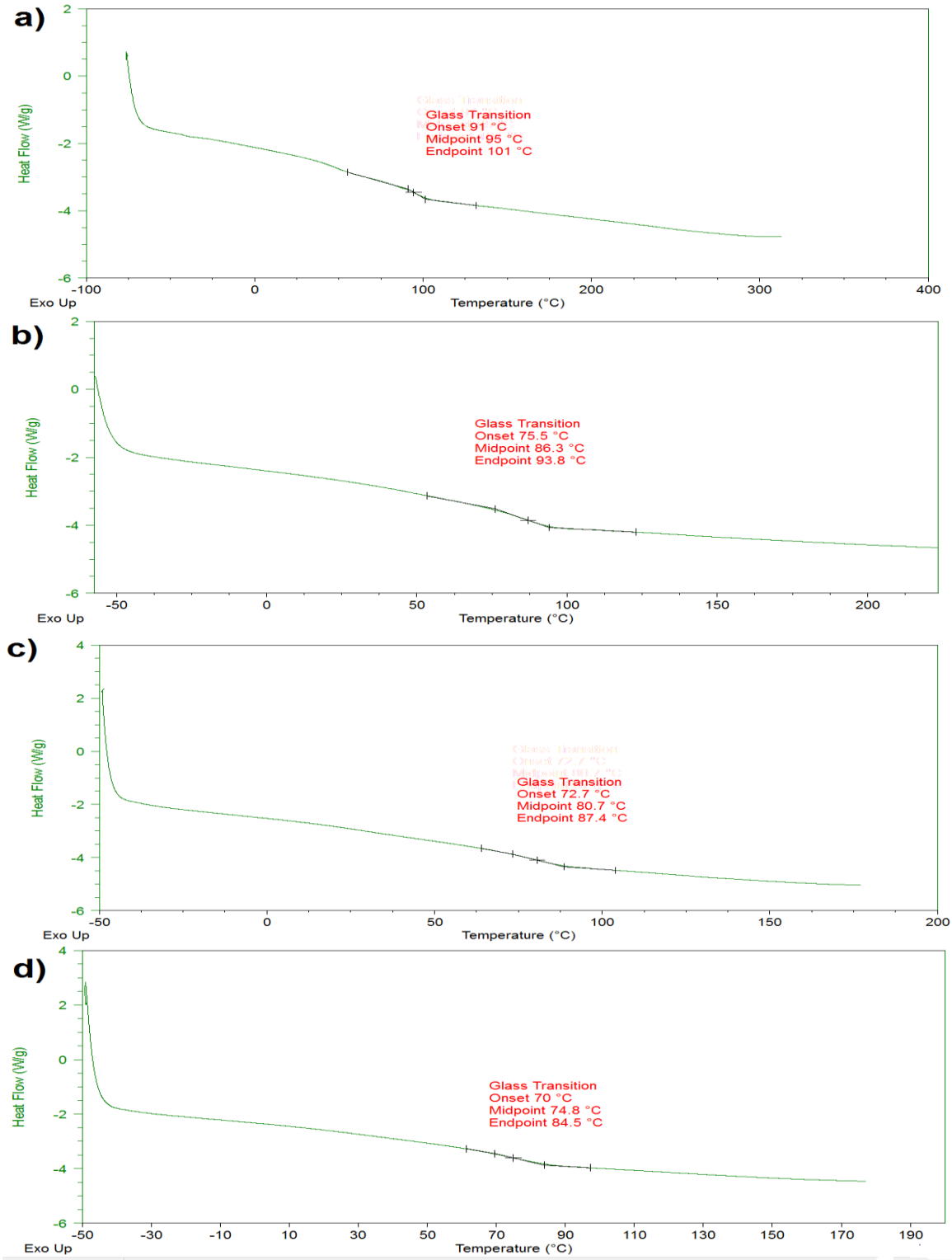

Figure 4.26: DSC curves of (a) 2, (b) 4, (c) 6 and (d) 8 wt.% SiO_2 nanocomposite coating systems

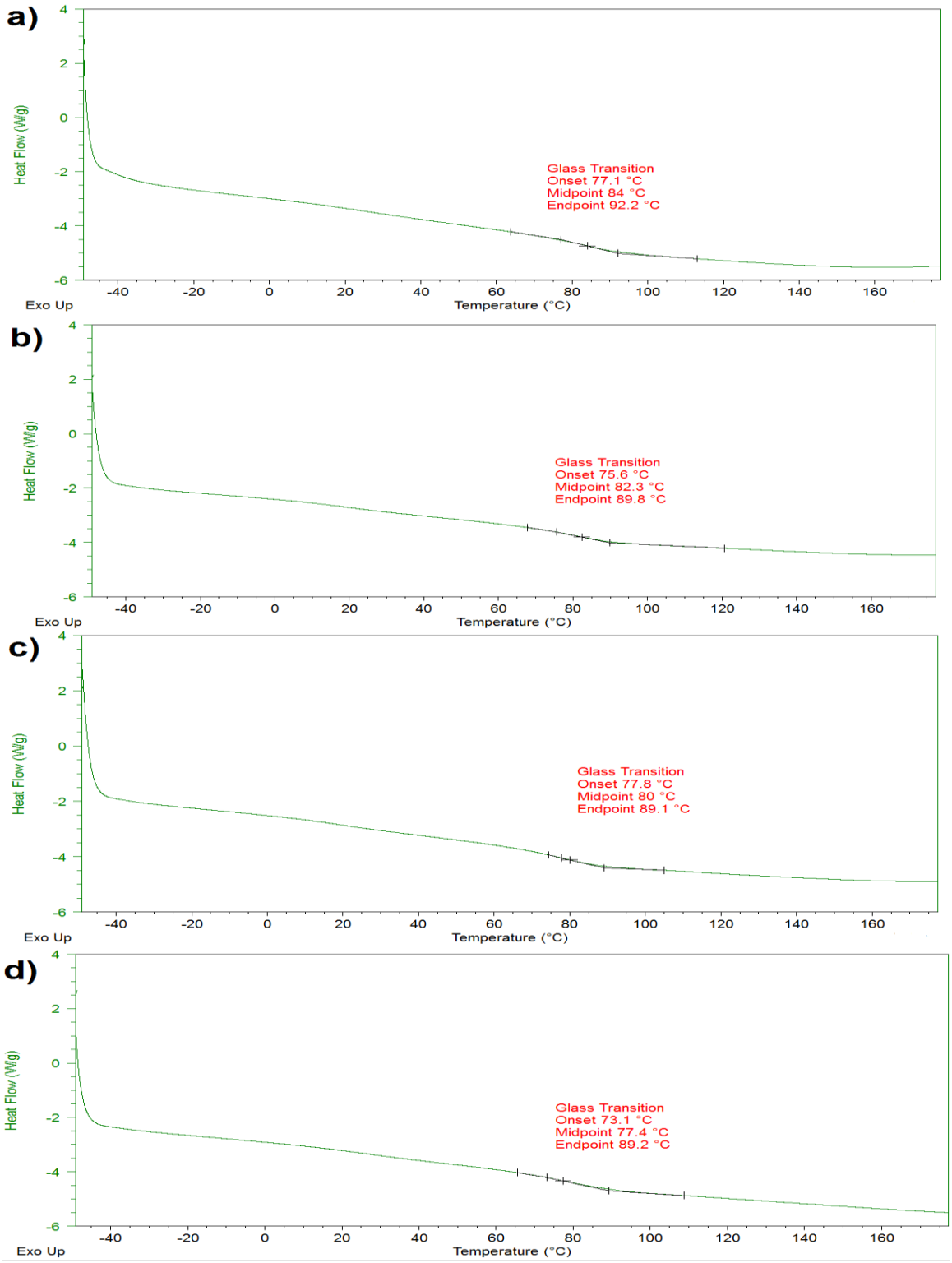

Figure 4.27: DSC curves of (a) 2, (b) 4, (c) 6 and (d) 8 wt.% ZnO nanocomposite coating systems

According to Figures 4.26 and 4.27, the T_g values of the developed organic-inorganic nanocomposite coating systems are significantly influenced by the presence of SiO_2 as well as ZnO nanoparticles. Testing the samples shows that using of 2 wt.% nano SiO_2 can increase the glass transition temperature up to 95°C. This improvement in the T_g value can be attributed, as mentioned by (Ramezanzadeh et al., 2011b) to the strong physical interactions that the nanoparticles can produce with the coating matrix. This effect of the nanoparticles appeared just for a low loading rate of SiO_2 nanoparticles. While on the contrary, nanocomposites reinforced with 4, 6 and 8 wt.% SiO_2 nanoparticles present a lowering effect on T_g that in turn can be related to the increment in the free volume caused by the nanoparticles. For nanocomposite coatings containing ZnO nano fillers, decreasing in T_g values is pronounced at all addition rates. The weak interactions among the particles and resin chains can be considered as one of the reasons behind the decrease of the T_g when reinforcing the polymeric matrix with nano ZnO particles. In addition, the weakness, in the mentioned interactions, may be attached to the poor ability of the agglomerated particles to provide strong interactions with the coating matrix (Ramezanzadeh & Attar, 2011).

It is worth to be mentioned that the size of the nano fillers, as well as the nanoparticles loading rates, play a vital role in the affecting the T_g. As example, SiO_2 with size ranging from 10 to 20 nm and with 2 wt.% addition amount have increased the T_g of the epoxy modified silicone coating while the same amount of ZnO nanoparticles with size of 100nm leads to decrease T_g.

4.7 Thermogravimetric analysis (TGA)

The TGA thermograms for all prepared samples are shown in Figures 4.28 and 4.29. For neat epoxy, silicone modified epoxy, SiO_2 nanocomposite and ZnO nanocomposite coatings, a double step decomposition was observed. Also, it can be seen that most significant weight loss occurred in the temperature range of 350–390 °C. Camino et al, (2005) have studied the thermal degradation of the epoxy resin and have concluded with that, the first step of degradation involves water elimination. That results in the production of C-C unsaturation. While the second step can be corresponded to an extensive breakdown of chemical bonds of the epoxy network including C-phenyl bonds of bisphenol-A.

The incorporation of hydroxyl terminated polydimethylsiloxane with epoxy resin enhances thermal stability and improves thermal degradation temperature (Velan & Bilal, 2000). The crosslinking between silicone and epoxy results in increasing the heat energy that required for reaching the same weight loss percentage that was noted for unmodified epoxy. In addition, the degradation of the coating system containing PDMS was delayed. That in turn can be attributed to the present of (–Si–O–Si–) of silicone structure which characterized by inorganic nature and could consider as the responsible for the stability enhancement. Ananda Kumar & Sankara Narayanan, (2002) have mentioned that the partial ionic nature of the silicone bond and its high energy are obviously responsible for its principal thermal stability.

Tables 4.9 and 4.10 show the temperatures that corresponded to 10, 20, 30 and 50% weight losses of the developed coating and nanocomposite systems. For instance, the 50 wt.% loss of neat epoxy was observed at approximately 375 °C. While, on the contrary, the same

percentage of the weight loss for the siliconized epoxy system was enhanced to 389 °C. Further, it is also observed that the variation of the temperatures values of the siliconized epoxy reinforced with either SiO_2 or ZnO nanoparticles is insignificant. However, a slight decreasing trend in the temperatures was noted when nano fillers were incorporated into the PDMS-epoxy matrix.

Table 4.9: The corresponded temperatures to different weight loss percentages of neat epoxy, PDMS-epoxy and SiO_2 nanocomposite coating systems

Weight Loss (%) / System	Temperature required to attain different weight losses (°C)					
	Neat epoxy	**PDMS-epoxy**	**2% SiO_2**	**4% SiO_2**	**6% SiO_2**	**8% SiO_2**
10	**351.7**	**353.9**	**351.5**	**353.3**	**350.1**	**351.4**
20	**352.3**	**354.4**	**352.3**	**354.1**	**351.3**	**352.4**
30	**352.6**	**356.4**	**354**	**355.7**	**354.1**	**354.6**
50	**375.5**	**389.1**	**379.4**	**381**	**378.3**	**381.6**

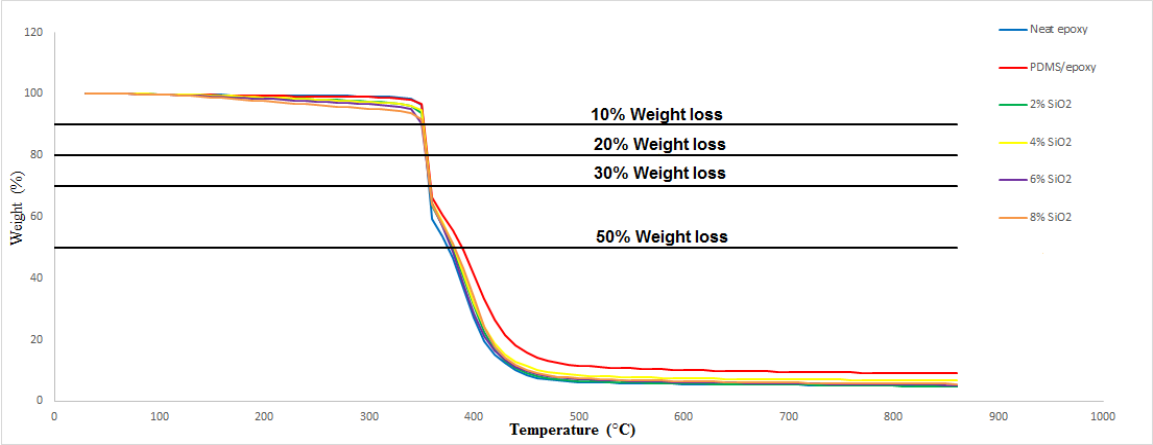

Figure 4.28: TGA thermograms of neat epoxy, PDMS-epoxy and SiO_2 nanocomposite coating systems and their corresponding weight loss percentages.

Table 4.10: The corresponded temperatures to different weight loss percentages of neat epoxy, PDMS/epoxy and ZnO nanocomposite coating systems

Weight Loss (%) / System	Temperature required to attain different weight losses (°C)					
	Neat epoxy	PDMS-epoxy	2% ZnO	4% ZnO	6% ZnO	8% ZnO
10	351.7	353.9	354.9	349	353.3	350.2
20	352.3	354.4	356.1	351.5	354.7	352.8
30	352.6	356.4	359.3	356.1	357.6	357.5
50	375.5	389.1	384.2	387.7	382.1	388.5

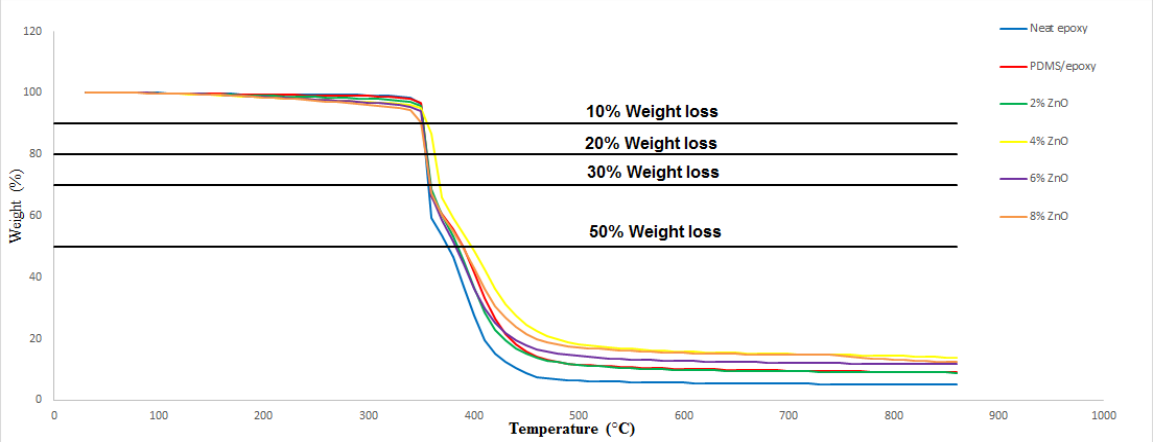

Figure 4.29: TGA thermograms of neat epoxy, PDMS-epoxy and ZnO nanocomposite coating systems and their corresponding weight loss percentages.

Chapter 5: Discussion

The most important component of the coating system is the resin. The quality of the coating film depends on the properties of the resin components. For a coating system to exhibit superior anti-corrosion performance, heat resistance and hydrophobic properties, the proper cross-linking among binder components must be achieved followed by developing a well dispersion of the second phase reinforcement additives within the matrix. It is the objective of this work to develop a durable cross-linked polymeric matrix consist of epoxy resin as the base and hydroxyl terminated –polydimethylsiloxane (HT-PDMS) as the modifier and study the effect of the two types of nanoparticles, SiO_2 and ZnO, on the overall performance of the nanocomposite coating systems.

The achieving of the hybrid organic-inorganic nanocomposite coatings was divided into two steps:

- First, PDMS-epoxy binder that acts as the polymeric matrix for the nano fillers was developed by the employment of cross-linking agent, 3-aminopropyltriethoxysilane, and dibutyltindilaurate catalyst. During the blending process, the amino group of the cross-linking agent first reacts with epoxide ring of the epoxy resin. This step was confirmed by FTIR spectra with the disappearance of the absorption peak at 915 cm^{-1}. The second step of the crosslinking process includes the observation of the at peaks 803 cm^{-1} and 1090 cm^{-1} in the silicone modified epoxy spectra. These peaks in turn corresponded to Si-C band and stretching of Si- O-Si band respectively. The observations mentioned above are the most significant results obtained from FTIR spectroscopy with the

indication of the vital role that the alkoxy group of g-aminopropyltriethoxysilane plays in promoting the reaction between epoxy and PDMS resins. Furthermore, FESEM image (Figure 4.7.b) further confirming the existence of inter cross-linked structure into the epoxy modified with PDMS system (Ananda Kumar & Sankara Narayanan, 2002).

- Secondly, embedding the nanoparticles within the polymeric matrix was carried out depending on the solution intercalation method. The nanoparticles in the powder form were first dissolved in xylene solvent in order to obtain swollen nanoparticles. The nanoparticles- solvent mixture and the prepared PDMS-epoxy binder were blended together. Then vaporization solvent process took place in order to achieve the intercalated nanocomposite by giving the ability to the polymer chains to diffuse between the layers of the swollen nanoparticles and sandwiching (Olad, 2011). FTIR results of SiO_2 nanocomposite coatings as well as ZnO nanocomposite coatings did not show any significant band shifts compared to PDMS-epoxy prepolymer. This trend of either SiO_2 nanoparticles or ZnO nanoparticles, confirm that the incorporation of nanoparticles in the modified silicone epoxy matrix did not affect the developed structure.

In this work, the contact angle measurements reveal that neat epoxy coating system showed hydrophilic nature. One of the objectives of this work, is to achieve hydrophobicity for the coated surfaces. Binder coatings developed by the incorporation of PDMS with the epoxy resin possessed water contact angle up to 96°. Further hydrophobicity enhancement was recorded when either SiO_2 or ZnO nanoparticles were embedded within the polymeric matrix.

Jiang et al., (2000) and Wang et al., (2011) have suggested that the improvement of the surface hydrophobicity could be through two possible methods. First, by changing the chemical composition of the coating, which in turn was clearly observed in the contact angle results of PDMS-epoxy coating system. The second method to reduce the wettability of the surface includes the effect of the topographic structure of the surface. By considering this concept, as the concentration of the nanoparticles in the coating films increases, the roughness of the surface increases. Bharathidasan et al., (2014) have mentioned that, the ability of the rough surface to present hydrophobic state can be attributed due to the formation of air pockets between water and the surface leading to composite solid-liquid-air interface.

From the contact angle results and FESEM images, it can be understood that the most pronounced effect of the SiO_2 nanoparticles, as well as ZnO nanoparticles, was observed with 6 wt.% loading ratio and this loading ratio had the most influence effect on the wettability of the nanocomposite coating system.

A good coating system must have high coating resistance. Coating resistance (R_c) in the order of 10^9 Ω and above expresses a good anti-corrosion performance of the coating system (Greenfield & Scantlebury, 2000; Ramesh et al., 2013; Rau et al ., 2012).

EIS data in the form of Bode and Nyquist plots were recorded from time to time over 30 days of immersion in 3% NaCl solution. For neat epoxy, coating resistance (R_c) value in the order of 10^5 Ω was recorded, which indicates the blister formation and corrosion initiation. But after the incorporation of PDMS in epoxy resin, R_c increased to 10^8 Ω over the same period of exposure. That again shows that the PDMS-epoxy coating system is justifying the objective of the present work.

Reinforcing the polymer matrix with nano-sized particles played a vital role in improving the barrier performance of the coating systems and enhancing the anti-corrosion performance. Ramezanzadeh et al., (2011) and Shi et al., (2009) have attributed the influence of the nanoparticles in the overall corrosion protection performance due to increasing the quality of the coating films by reducing the porosity and zigzagging the diffusion pathways. Also, by improving the adherence and due to the physical nature of the interactions between the nanoparticles and the polymeric matrix, compared to the chemical interaction among the resin chains, which can consider more efficient in improving the resistance against the hydrolytic degradation.

Both SiO_2 and ZnO nanoparticles affected in the same way in improving the coating resistance during the 30 days of immersion. 2 wt.% and 4 wt.% nanoparticles loading rates within PDMS-epoxy matrix perform superior corrosion protection with $R_c > 10^9$ Ω. While, on the contrary, as the amount of the nanoparticles increased, especially above 4 wt.%, the cross-linking density decreased. That in turn shows complete agreement with T_g results. In addition, the decreasing in the R_c values, of the coating systems with 6 wt.% and 8 wt.% of SiO_2 or ZnO nanoparticles, was explained by Ramezanzadeh et al., (2011b) as the high tendency of the nanoparticles to form aggregations at high loading rates. That also has been confirmed by FESEM images in Figure (4.8 c and d) and Figure (4.9 c and d).

From DSC studies, it is observed that T_g increased after the epoxy modification with PDMS resin. The higher T_g value of PDMS-epoxy coating could be due to the higher degree of crosslinking which in turn leads to low free volume concentration as the molecules close up during the curing process. Additionally, the FESEM image that is shown in Figure 4.7.b

confirms the existence of inter crosslinking structure of epoxy modified with PDMS system (Ananda Kumar & Sankara Narayanan, 2002).

Except the coating containing 2 wt.% of SiO_2 nanoparticles, all other loading rates of SiO_2 and ZnO nanoparticles incorporated nanocomposite coatings showed decreasing in the T_g value. Ramezanzadeh et al., (2011) have mentioned that, the nanoparticles could produce strong physical interactions with the coating matrix which implies that the sample with 2 wt.% of SiO_2 nanoparticles has lower flexibility and, therefore, higher T_g. Whereas, the decreasing in T_g values, obtained from the addition of nano SiO_2 > 2 wt.% or the addition of ZnO nanoparticles, can be attributed to the increasing in the free volume and the decreasing in the cross-linking density caused by the incorporation of the nanoparticles in the polymeric matrix.

TGA studies showed that the thermal degradation of all samples occurred in two major stages, and most significant weight loss occurs in the temperature range of 350–390 °C. The first weight loss is attributed to elimination of moisture or water content by heating. While the second step can be corresponded to an extensive breakdown of chemical bonds of the epoxy network including C-phenyl bonds of bisphenol-A (G. Camino et al., 2005).

The incorporation of PDMS into the epoxy resin results in forming (–Si–O–Si–) band which was previously confirmed in FTIR spectra by the observation of the peak at 1090 cm^{-1}. This band in turn characterized by inorganic nature and consider as the responsible for the thermal stability enhancement. Ananda Kumar & Sankara Narayanan, (2002) have suggested that the partial ionic nature of the silicone bond and its high energy are obviously

responsible for its principal thermal stability. Insignificant changes occurred in the thermograms of the SiO_2 nanocomposites as well as ZnO nanocomposites which confirm the ability of the coatings to withstand temperatures even after the addition of the nanoparticles.

Based on the results obtained, it can be conclusively said that the incorporation of PDMS with epoxy resin enhances the quality of the coating system. Furthermore, reinforcing the developed PDMS-epoxy matrix with nano-sized particles shows a prominent improvement in the anti-corrosion performance and significantly enhancing the hydrophobicity of the surface. It is worth to be mentioned that 2 wt.% loading ratio of SiO_2 nanoparticles had the most pronounced enhancement of all coating properties. Likewise, the system with 2 wt.% of ZnO nanoparticles shows the best results comparing to other ZnO nanocomposite coating systems. From the present investigations, it can be deduced that the nanocomposite system with just 2 wt.% of nanoparticles exhibits an economic usability in the manufacturing application of the nanocomposite anticorrosion coating systems.

Chapter 6: Conclusions and suggestions for future works

6.1 Conclusions

In this study, PDMS-epoxy blend has been prepared using 3-aminopropyltriethoxy silane cross-linking agent, dibutyltindilaurate catalyst and polyamide curing agent. 10 wt.% of PDMS was successfully utilized to modify epoxy resin in order to obtain the proper polymeric matrix that will be used as the host for the reinforcing nanoparticles.

It was observed that the presence of polydimethylsiloxane (PDMS) enhances the anti-corrosion properties of epoxy resin. In addition, hydrophobic character was recorded for the surface when 10 wt.% :90 wt.% of PDMS: epoxy applied to cold roll steel panels. DSC and TGA results of silicone modified epoxy coating systems show that the thermal properties were significantly enhanced comparing to the neat epoxy coating system.

The hybrid organic - inorganic nanocomposite coating systems were developed by the employment of the solution intercalation method for the purpose of introducing the reinforcing nanoparticles to the developed PDMS-epoxy polymeric matrix. The effects of the incorporation of SiO_2, as well as ZnO, nanoparticles with the formed binder can be described as follows:

- FTIR spectra of the nanocomposite samples with no significant changes were recorded. That in turn can be attributed to the physical nature of the interactions between the nano-sized particles and the polymeric matrix.

- Well dispersion of the nanoparticles within the matrix was confirmed through the morphology studies. It has been seen in FESEM images that the addition of the

nanoparticles leads to increasing the surface roughness. The investigations also showed that there was a high tendency of the nanoparticles to form aggregations at the high loading rates especially at 8 wt.%.

- Significant effects on the hydrophobicity of the coated surface were observed. The addition of SiO_2 or ZnO particles was able to increase the roughness of the surface which in turn leads to promote the hydrophobicity by forming air pockets between the water and the surface leading to composite solid-liquid-air interface. Thus, it was found that the water contact angle of the SiO_2 nanocomposite and ZnO nanocomposite samples had much higher value comparing to unreinforced samples.

- The vital role of the nanoparticles was clearly observed in EIS results. A superior anti-corrosion performance with excellent barrier behavior were noted for the nanocomposite coating systems. It was found that 2 wt.% of either SiO_2 or ZnO nanoparticles could be enough to make the coating film withstand the corrosive environment. Systems with 2 wt.% of nanoparticles loading ratio show coating resistance (R_c) in the order of approximately 10^{11} Ω up to 30 days of immersion in 3% NaCl solution. That in turn indicates that the incorporation of nanoparticles in the polymeric matrix had increased the overall corrosion protection performance of the developed coatings.
- A slight decreasing in the crosslinking density was observed after embedding SiO_2 or ZnO nanoparticles with PDMS-epoxy binder. More flexibility and lower T_g values were recorded as the addition amount of the nanoparticles increased. It is worth to be

mentioned that the coating system with 2 wt.% SiO_2 nanoparticles influenced in different way on the glass transition temperature. This in turn could be attributed due to the strong physical interaction with the polymeric matrix produced by the low concentration of SiO_2 nanoparticles.

- TGA results did not show any significant changes after the addition of the nanoparticles to the polymeric matrix.

Characterization of PDMS-epoxy coating system and investigate the effects of the incorporation of either SiO_2 or ZnO nanoparticles, with different weight ratios, into the developed polymeric matrix have been done. One can conclude that, the nanocomposite coatings developed in this study are suitable for numerous applications. The novelty of this work lies in the development of hybrid organic - inorganic binder and reinforcing it with particles in the nano-scale. As mentioned in earlier chapters, the number one objective of this work is to develop organic-inorganic nanocomposite coating systems consist of epoxy and silicone with nanoparticles has been achieved. EIS and water contact angle measurements have illustrated the effects of the nanoparticles on the wettability and electrochemical properties which confirm the fulfillment of the objective number two. FTIR and FESEM gave a full understanding of the structure and the morphology of the developed systems. In addition, the thermal properties were investigated by DSC and TGA techniques. These showed that the objective number three is fulfilled.

6.2 Suggestions for Future Works

Future work should concentrate on making or searching for binders and nanocomposites that are more friendly to the environment by the using of water-borne resins with low cost, non-toxic and good protection ability. The incorporation of the nanoparticles within PDMS-epoxy resin seems to improve the hydrophobicity. Thus, further improving in the hydrophobicity of the surface should take place in order to achieve a super-hydrophobic coatings and study the effect of this character on the anti-corrosion performance of the system.

References

Ahmad, S., Gupta, A., Sharmin, E., Alam, M., & Pandey, S. (2005). Synthesis, characterization and development of high performance siloxane-modified epoxy paints. *Progress in Organic Coatings, 54*(3), 248-255.

Akbarinezhad, E., Rezaei, F., & Neshati, J. (2008). Evaluation of a high resistance paint coating with EIS measurements: Effect of high AC perturbations. *Progress in Organic Coatings, 61*(1), 45-52.

Amerio, E., Fabbri, P., Malucelli, G., Messori, M., Sangermano, M., & Taurino, R. (2008). Scratch resistance of nano-silica reinforced acrylic coatings. *Progress in Organic Coatings, 62*(2), 129-133.

Amirudin, A., & Thierry, D. (1995). Application of electrochemical impedance spectroscopy to study the degradation of polymer-coated metals. *Progress in Organic Coatings, 26*(1), 1-28.

Ananda Kumar, S., & Sankara Narayanan, T. (2002). Thermal properties of siliconized epoxy interpenetrating coatings. *Progress in Organic Coatings, 45*(4), 323-330.

Bagherzadeh, M., & Mousavinejad, T. (2012). Preparation and investigation of anticorrosion properties of the water-based epoxy-clay nanocoating modified by Na^{+} -MMT and Cloisite 30B. *Progress in Organic Coatings, 74*(3), 589-595.

Bharathidasan, T., Kumar, S. V., Bobji, M., Chakradhar, R., & Basu, B. J. (2014). Effect of wettability and surface roughness on ice-adhesion strength of hydrophilic, hydrophobic and superhydrophobic surfaces. *Applied Surface Science, 314*, 241-250.

Camino, G., Tartaglione, G., Frache, A., Manferti, C., & Costa, G. (2005). Thermal and combustion behaviour of layered silicate–epoxy nanocomposites. *Polymer Degradation and Stability, 90*(2), 354-362.

Castela, A., & Simoes, A. (2003). Assessment of water uptake in coil coatings by capacitance measurements. *Progress in Organic Coatings, 46*(1), 55-61.

Chen, H. R., Shi, J. L., Li, Y. S., Yan, J. N., Hua, Z. L., Chen, H. G., & Yan, D. S. (2003). A new method for the synthesis of highly dispersive and catalytically active platinum nanoparticles confined in mesoporous zirconia. *Advanced Materials, 15*(13), 1078-1081.

Chew, K., Yahaya, A., & Arof, A. (2000). Studies on the properties of silicone resin films on mild steel. *Pigment & resin technology, 29*(6), 364-368.

Dodiuk, H., & Goodman, S. H. (2013). *Handbook of thermoset plastics*: William Andrew.

Dolatzadeh, F., Moradian, S., & Jalili, M. M. (2011). Influence of various surface treated silica nanoparticles on the electrochemical properties of SiO< sub> 2</sub>/polyurethane nanocoatings. *Corrosion Science, 53*(12), 4248-4257.

Duo, S., Li, M., Zhu, M., & Zhou, Y. (2008). Polydimethylsiloxane/silica hybrid coatings protecting Kapton from atomic oxygen attack. *Materials Chemistry and Physics, 112*(3), 1093-1098.

Enns, J. B., & Gillham, J. K. (1983). Time–Temperature–Transformation (TTT) cure diagram: Modeling the cure behavior of thermosets. *Journal of Applied Polymer Science, 28*(8), 2567-2591.

Forsgren, A. (2006). *Corrosion control through organic coatings*: CRC Press.

Garcia, F. G., & Soares, B. G. (2003). Determination of the epoxide equivalent weight of epoxy resins based on diglycidyl ether of bisphenol A (DGEBA) by proton nuclear magnetic resonance. *Polymer Testing, 22*(1), 51-56.

Ghaemy, M., & Riahy, M. (1996). Kinetics of anhydride and polyamide curing of bisphenol A-based diglycidyl ether using DSC. *European Polymer Journal, 32*(10), 1207-1212.

González, S., Mirza Rosca, I., & Souto, R. (2001). Investigation of the corrosion resistance characteristics of pigments in alkyd coatings on steel. *Progress in Organic Coatings, 43*(4), 282-285.

Greenfield, D., & Scantlebury, D. (2000). The protective action of organic coatings on steel: a review. *Journal of Corrosion Science & Engineering, 3*.

Grundmeier, G., Schmidt, W., & Stratmann, M. (2000). Corrosion protection by organic coatings: electrochemical mechanism and novel methods of investigation. *Electrochimica Acta, 45*(15), 2515-2533.

Heidarian, M., Shishesaz, M., Kassiriha, S., & Nematollahi, M. (2010). Characterization of structure and corrosion resistivity of polyurethane/organoclay nanocomposite coatings prepared through an ultrasonication assisted process. *Progress in Organic Coatings, 68*(3), 180-188.

Heidarian, M., Shishesaz, M., Kassiriha, S., & Nematollahi, M. (2011). Study on the effect of ultrasonication time on transport properties of polyurethane/organoclay nanocomposite coatings. *Journal of Coatings Technology and Research, 8*(2), 265-274.

Hou, S.-S., Chung, Y.-P., Chan, C.-K., & Kuo, P.-L. (2000). Function and performance of silicone copolymer. Part IV. Curing behavior and characterization of epoxy–siloxane copolymers blended with diglycidyl ether of bisphenol-A. *Polymer, 41*(9), 3263-3272.

Huttunen-Saarivirta, E., Vaganov, G., Yudin, V., & Vuorinen, J. (2013). Characterization and corrosion protection properties of epoxy powder coatings containing nanoclays. *Progress in Organic Coatings, 76*(4), 757-767.

Jiang, L., Wang, R., Yang, B., Li, T., Tryk, D., Fujishima, A., . . . Zhu, D. (2000). Binary cooperative complementary nanoscale interfacial materials. *Pure and Applied Chemistry, 72*(1-2), 73-81.

Kanungo, M., Mettu, S., Law, K.-Y., & Daniel, S. (2014). Effect of Roughness Geometry on Wetting and Dewetting of Rough PDMS Surfaces. *Langmuir, 30*(25), 7358-7368.

Kapridaki, C., & Maravelaki-Kalaitzaki, P. (2013). TiO_2<–SiO_2–PDMS nano-composite hydrophobic coating with self-cleaning properties for marble protection. *Progress in Organic Coatings, 76*(2), 400-410.

Kumar, S. A., Alagar, M., & Mohan, V. (2002). Studies on corrosion-resistant behavior of siliconized epoxy interpenetrating coatings over mild steel surface by electrochemical methods. *Journal of Materials Engineering and Performance, 11*(2), 123-129.

Matin, E., Attar, M., & Ramezanzadeh, B. (2015). Investigation of corrosion protection properties of an epoxy nanocomposite loaded with polysiloxane surface modified nanosilica particles on the steel substrate. *Progress in Organic Coatings, 78*, 395-403.

Montemor, M. (2014). Functional and smart coatings for corrosion protection: A review of recent advances. *Surface and Coatings Technology*.

Nematollahi, M., Heidarian, M., Peikari, M., Kassiriha, S., Arianpouya, N., & Esmaeilpour, M. (2010). Comparison between the effect of nanoglass flake and montmorillonite organoclay on corrosion performance of epoxy coating. *Corrosion Science, 52*(5), 1809-1817.

Nguyen, T. N., Hubbard, J. B., & MCFADDEN, G. B. (1991). A mathematical model for the cathodic blistering of organic coatings on steel immersed in electrolytes. *JCT, Journal of coatings technology, 63*(794), 43-52.

Nikolic, G., Zlatkovic, S., Cakic, M., Cakic, S., Lacnjevac, C., & Rajic, Z. (2010). Fast fourier transform IR characterization of epoxy GY systems crosslinked with aliphatic and cycloaliphatic EH polyamine adducts. *Sensors, 10*(1), 684-696.

Olad, A. (2011). Polymer/clay nanocomposites. *Advances in diverse industrial applications of nanocomposites*, 113-138.

Pascault, J.-P., & Williams, R. J. (2009). *Epoxy polymers*: John Wiley & Sons.

Pouget, E., Tonnar, J., Lucas, P., Lacroix-Desmazes, P., Ganachaud, F., & Boutevin, B. (2009). Well-architectured poly (dimethylsiloxane)-containing copolymers obtained by radical chemistry. *Chemical Reviews, 110*(3), 1233-1277.

Ramesh, K., Nor, N., Ramesh, S., Vengadaesvaran, B., & Arof, A. (2013). Studies on Electrochemical Properties and FTIR analysis of Epoxy Polyester Hybrid Coating System. *Int. J. Electrochem. Sci, 8*, 8422-8432.

Ramezanzadeh, B., & Attar, M. (2011). Characterization of the fracture behavior and viscoelastic properties of epoxy-polyamide coating reinforced with nanometer and micrometer sized ZnO particles. *Progress in Organic Coatings, 71*(3), 242-249.

Ramezanzadeh, B., Attar, M., & Farzam, M. (2011a). Effect of ZnO nanoparticles on the thermal and mechanical properties of epoxy-based nanocomposite. *Journal of Thermal Analysis and Calorimetry, 103*(2), 731-739.

Ramezanzadeh, B., Attar, M., & Farzam, M. (2011b). A study on the anticorrosion performance of the epoxy–polyamide nanocomposites containing ZnO nanoparticles. *Progress in Organic Coatings, 72*(3), 410-422.

Rau, S. R., Vengadaesvaran, B., Ramesh, K., & Arof, A. (2012). Studies on the Adhesion and Corrosion Performance of an Acrylic-Epoxy Hybrid Coating. *The Journal of Adhesion, 88*(4-6), 282-293.

Saji, V. S., & Cook, R. (2012). *Corrosion protection and control using nanomaterials*: Elsevier.

Sharmin, E., Imo, L., Ashraf, S. M., & Ahmad, S. (2004). Acrylic-melamine modified DGEBA-epoxy coatings and their anticorrosive behavior. Progress in organic coatings, 50(1), 47-54.

Shi, X., Nguyen, T. A., Suo, Z., Liu, Y., & Avci, R. (2009). Effect of nanoparticles on the anticorrosion and mechanical properties of epoxy coating. Surface and Coatings Technology, 204(3), 237-245.

Soer, W. J., Ming, W., Koning, C., van Benthem, R., Mol, J., & Terryn, H. (2009). Barrier and adhesion properties of anti-corrosion coatings based on surfactant-free latexes from anhydride-containing polymers. *Progress in Organic Coatings, 65*(1), 94-103.

Sørensen, P. A., Kiil, S., Dam-Johansen, K., & Weinell, C. (2009). Anticorrosive coatings: a review. *Journal of Coatings Technology and Research, 6*(2), 135-176.

Su, C., Li, J., Geng, H., Wang, Q., & Chen, Q. (2006). Fabrication of an optically transparent super-hydrophobic surface via embedding nano-silica. *Applied Surface Science, 253*(5), 2633-2636.

Sun, L., Boo, W.-J., Clearfield, A., Sue, H.-J., & Pham, H. (2008). Barrier properties of model epoxy nanocomposites. *Journal of Membrane Science, 318*(1), 129-136.

Téllez, L., Rubio, J., Rubio, F., Morales, E., & Oteo, J. (2004). FT-IR Study of the Hydrolysis and Polymerization of Tetraethyl Orthosilicate and Polydimethyl Siloxane in the Presence of Tetrabutyl Orthotitanate. *Spectroscopy Letters, 37*(1), 11-31.

Velan, T. T., & Bilal, I. M. (2000). Aliphatic amine cured PDMS-epoxy interpenetrating network system for high performance engineering applications—Development and characterization. *Bulletin of Materials Science, 23*(5), 425-429.

Wang, S., Li, Y., Fei, X., Sun, M., Zhang, C., Li, Y., . . . Hong, X. (2011). Preparation of a durable superhydrophobic membrane by electrospinning poly (vinylidene fluoride)(PVDF) mixed with epoxy–siloxane modified SiO 2 nanoparticles: a possible route to superhydrophobic surfaces with low water sliding angle and high water contact angle. *Journal of Colloid and Interface Science, 359*(2), 380-388.

Wicks Jr, Z. W., Jones, F. N., Pappas, S. P., & Wicks, D. A. (2007). *Organic coatings: science and technology*: John Wiley & Sons.

Zhang, S., Sun, D., Fu, Y., & Du, H. (2003). Recent advances of superhard nanocomposite coatings: a review. Surface and Coatings Technology, 167(2), 113-119.

Zhou, S., Wu, L., Sun, J., & Shen, W. (2002). The change of the properties of acrylic-based polyurethane via addition of nano-silica. *Progress in Organic Coatings, 45*(1), 33-42.